

Barotropic theory for the velocity profile of Jupiter turbulent jets: an example for an exact turbulent closure

E. Woillez¹, and F. Bouchet^{†1}

¹Univ Lyon, Ens de Lyon, Univ Claude Bernard, CNRS, Laboratoire de Physique, F-69342 Lyon, France

(Received xx; revised xx; accepted xx)

We model the dynamics of Jupiter's jets by averaging the dynamics of eddies, in a barotropic beta-plane model, and explicitly predicting the balance between Reynolds' stresses and dissipation, thus predicting the average velocity profile explicitly. In order to obtain this result, we adopt a non-equilibrium statistical mechanics approach. We consider a relevant limit for Jupiter troposphere, of a time scale separation between inertial dynamics on one hand, and stochastic forcing and dissipation on the other hand. We assume that the forcing acts on scales much smaller than the jet scale, and we obtain a very simple explicit relation between the Reynolds stress, the energy injection rate, and the average velocity shear, valid far from the jet edges (extrema of zonal velocity). A specific asymptotic expansion close to jet edges unravel an asymmetry between eastward and westward, velocity extrema. We recover Jupiter's jet specificities: a cusp on eastward jets and a smooth parabola on westward jets.

Key words: Authors should not enter keywords on the manuscript, as these must be chosen by the author during the online submission process and will then be added during the typesetting process (see <http://journals.cambridge.org/data/relatedlink/jfm-keywords.pdf> for the full list)

1. Introduction

The giant gaseous planets like Jupiter and Saturn can be seen as experimental systems to study geostrophic turbulent flows (see the review (Vasavada & Showman 2005) for Jupiter). The data collected by the probes Galileo and Cassini during their close encounter with Jupiter gave high resolution observations of the dynamics of the upper layers of Jupiter's atmosphere (Salyk *et al.* 2006; Porco *et al.* 2003). Not only do we have access to the velocity profile of zonal winds that form the alternance of large colored bands at the top of the troposphere, but we also have a lot of informations of the smaller vortices imbedded in the flow. Those vortices often appear after three dimensional convective activity in the atmosphere. Those fluctuations of the wind are continuously injecting energy to the zonal wind (Ingersoll *et al.* 1981; Salyk *et al.* 2006), and equilibrate the dissipation mechanisms. As the ratio between vertical and horizontal velocities is very small for those planets, the dynamics of the atmosphere, and the formation of large scale jets, may be qualitatively well understood within the framework of two-dimensional

[†] Email address for correspondence: freddy.bouchet@ens-lyon.fr

geostrophic turbulence in a β plane (Pedlosky 1982), although more refined models are needed if one wants to understand the quantitative features of zonal jets on Jupiter (Li *et al.* 2006; Schneider & Liu 2009). As the aim of this work is to make progresses in the theoretical understanding of turbulent flows, we consider geostrophic turbulence in a β plane model. Despite all its limitations, for instance the lack of dynamical effects related to baroclinic instabilities, we will show that this model reproduces the main qualitative features of the velocity profiles.

An interesting property of two dimensional turbulent flows is their inverse energy transfer from small scales to large scales, sometimes through a cascade among scales, but much more often through a direct transfer from small scale to large scale mediated by the large scale flow. This inverse energy transfer is responsible for the self organization of the flow into large scale coherent structures that evolve much slower than the eddies. Among those structures, giant vortices and zonal jets have raised strong interest in the scientific community. The formation of those large scale structures is subtle and far from being perfectly understood. The β effect favors the formation of jets, but without β effect both jets and vortices can be observed in numerical simulations (Sommeria 1986; Frishman *et al.* 2017). Both structures are also observed in the atmosphere of gaseous planets (Ingersoll 1990; Galperin *et al.* 2014, 2001). On Earth, jets play a crucial role in atmosphere dynamics and their analysis is one of the key for understanding climate dynamics. From a theoretical point of view, the dynamics of turbulent jets and vortices is still very challenging. Some years ago, the computation of statistical equilibrium theory of the two-dimensional Euler and quasi-geostrophic equations (Bouchet & Venaille 2012), using large deviation theory, led to the conclusion that zonal jets as well as large vortices are stable equilibrium states of the flow, and thus natural attractors. However, planetary flows are continuously forced with an energy injection at small scales and damped by many dissipative phenomena and are thus rather out of equilibrium systems. There is clear empirical and numerical evidence that quasi stationary states of non-equilibrium turbulent flows are nearly always close to statistical equilibria (Bouchet & Simonnet 2009), in the limit of time scale separation between force and dissipation on one hand, and inertial effects on the other hand. However a complete theoretical relation between the equilibrium states and the non-equilibrium states remains to be fully established. This work is one step in this direction.

Following the observation that zonal jets on Jupiter are forced by convective motion that are not described by the β plane model, it will be natural to model the forcing by stochastic forces. Adding stochastic forces is also a classical way to model such out of equilibrium systems. Thanks to the astronomical observations (Ingersoll *et al.* 1981; Salyk *et al.* 2006), we can estimate the magnitude of the parameters used in such a nonequilibrium models. It comes out that, provided we model Jupiter's jets by a beta plane model, the regime of weak forcing and weak dissipation is the relevant one. Moreover the convective plumes produce small vortices with a typical scale of order of few thousands kilometers, comparable with the the first internal Rossby deformation radius. This scale is thus much smaller than the typical meridional extension of jets, such that a small scale forcing limit may also be relevant.

One crucial question is to know whether simpler equations can be derived from the beta-plane turbulence ones, leading to a much deeper understanding. A promising nonequilibrium statistical theory is the stochastic structural stability (S3T) theory (Farrell & Ioannou 2003; Farrell & Ioannou 2007) or the closely related second order cumulant expansion theory (CE2) (Marston *et al.* 2008). The key ingredient in those theories is to neglect eddy-eddy interactions, keeping only the interaction between eddies and the mean flow. With this approximation, there is no inverse energy cascade in Fourier

space any more, and the inverse energy flux goes through interactions with the mean flow. This may be relevant only when the inverse energy cascade flux are negligible. In other intermediate case where the two inverse energy transfer phenomena do coexist, this drawback is corrected by a parametrization of the Fourier spectrum of the stochastic forcing (Farrell & Ioannou 1993). The flow governed by the S3T equations, with or without phenomenological added stochastic forcing, produces spontaneous emergence and equilibration of zonal jets (Bakas & Ioannou 2013; Constantinou *et al.* 2012) which velocity profiles reproduce quite well the main features of jets obtained in rotating-tank experiments (Read *et al.* 2004), numerical experiments (Vallis & Maltrud 1993; Williams 1978) or in the atmosphere of gaseous planets.

The question why quasilinear approximation give such good results has been addressed in (Bouchet *et al.* 2013). The main result of this work is to show that the quasilinear approximation is self-consistent in the limit of weak stochastic forcing and dissipation. Moreover it follows from this analysis that the quasilinear equations are expected to be valid above a crossover scale, that tends to zero in the limit of weak stochastic forces and dissipation limit. Using this justified approximation, it is then possible to write a *close* equation for the evolution of the mean velocity. This equation involves an abstract functional $F[U]$ that contains the effect of the small-scale turbulence on the mean flow. Even if this partial differential equation has no explicit solution, it is an important starting point for further numerical and theoretical studies, and it will be extensively used in the present work. We will show that a huge simplification occurs in the limit of small scale forcing.

The exact shape of zonal winds on Jupiter reveals an astonishing asymmetry between eastward jets and westward jets (Porco *et al.* 2003; Sánchez-Lavega *et al.* 2008; Garcí *et al.* 2001). Whereas eastward jets form cusps at their maximum velocity, westward jets are smoother, close to a parabolic velocity profile. At the same time, the profile of potential vorticity (PV) looks like “staircases” (Dritschel & McIntyre 2008), and all those prominent features are well reproduced in direct numerical simulations of β plane turbulence and with the S3T model. The “staircase” shape of potential vorticity could be a consequence of Rossby waves breaking, a phenomenon that mixes potential vorticity between two maxima of jets. Nevertheless, the physical mechanism leading to the staircase profile remains unclear. One could ‘postulate’ a PV staircase profile and derive the corresponding mean flow (Dritschel & McIntyre 2008), but we would like to have more insights in the mechanism of two-dimensional turbulence.

The aim of stochastic models is to give a close system of equations to study the dynamics of zonal jets. As we said, a theoretical model like for example the S3T model can be used to study the dynamics of the mean flow, but one still has to resolve together the dynamics of fluctuations of the velocity field. From a theoretical point of view, even the S3T system remains complicated. Even if it provides excellent framework to study numerically the dynamics of the flow (Constantinou 2015), it is a difficult work to emphasize the physical phenomena that lead to emergence and equilibration of a jet, because those phenomena are in some sense “hidden” by the numerical integration, and difficult to isolate. Another approach is to start directly from the equations and do analytic calculations. The kinetic theory developed in (Bouchet *et al.* 2013) has led to the justification of the quasilinear approximation and has emphasized the importance of the small parameter α that sets the magnitude of energy injection (Bouchet & Simonnet 2009). One year later, using a completely different approach, a way has been found (Laurie *et al.* 2014) to close the equation for the mean velocity, in the analogous problem of the two-dimensional stochastic Navier-Stokes equations. The energy balance for the eddies is composed of terms of different orders: some terms are quadratic in the fluctuations,

some are cubic, and there is a term involving the pressure. If the pressure term and the cubic terms are neglected, the surprising fact is that the Reynolds stress can be expressed in terms of the zonal velocity profile and the rate of energy injected in the flow. The consequence of this approximation is that, if a large scale vortex (Laurie *et al.* 2014) or a large scale jet (Falkovich 2016) is created, it should surprisingly exhibit a universal velocity profile, i.e a velocity profile that depends only on the energy injection rate. Such a universal velocity profile has indeed been observed in numerical simulations, in a restricted part of the domain, far from the core of the vortex and far from the flow separatrix. (Kolokolov & Lebedev 2016a) give scaling arguments to show in which domain of the flow the theoretical expression for the velocity profile is expected to hold. related to this theoretical work, detailed numerical studies of the energy balance has been discussed in several papers (Tangarife 2015; Nardini & Tangarife 2016; Frishman *et al.* 2017). One major contribution of this paper is, we hope, to give a unified framework that links the previous numerical and theoretical studies on zonal jets.

In this paper, following the work of (Bouchet *et al.* 2013) and (Laurie *et al.* 2014), we try to give a deeper physical understanding of the mechanisms leading to equilibration of a jet. Preliminary results related to the present work were obtained in (Woillez & Bouchet 2017). The present work contains partial analytical results, and numerical computations are performed when necessary to proceed in the analysis of the jet. Starting from the equations for a barotropic flow on a periodic beta plane with stochastic forces in section 2, we first write the energy balance for the mean flow and for the small scales of the flow. If, as a first guess, we assume that the energy injection rate at small scales per unit of mass ϵ ($m^2.s^{-3}$) is locally transferred to the mean flow U , and we neglect small scale dissipation and pressure effects, it happens that we can give an expression for the Reynolds stress that does not depend on the details of the stochastic forcing. It writes

$$\langle uv \rangle = \frac{\epsilon}{U}. \quad (1.1)$$

This expression is very similar to the one obtained in (Laurie *et al.* 2014) for a vortex. If the mean flow is linear, i.e U' is constant, it is possible to compute the Reynolds stress without approximations (Srinivasan & Young 2014). A similar result holds in the case of dipoles for the 2D Navier-Stokes equations (Kolokolov & Lebedev 2016a,b). The result can be expressed with the energy injection rate, the dissipation, the constant derivative U' and a parameter depending on the anisotropy of the stochastic forcing. In the limit of vanishing dissipation and fully anisotropic forcing, one finds expression (1.1). A first aim of this paper is to prove that this result can be recovered analytically with the quasilinear barotropic model, thus justifying the assumption that all energy is locally transferred in space to largest scales, and thus pressure effects are negligible. The quasilinear approximation and the pseudo-momentum conservation law allows us to give an expression for the divergence of the Reynolds stress (see equation (2.12)). In section 3, we carry out an asymptotic calculation of the Reynolds stress by taking the limit of small scale forcing first, and then taking the inertial limit (i.e vanishing linear friction). With those two limits, we recover expression (1.1).

In the following (section 3.2), we use the previous result (1.1) to write a *close* partial differential equation for the mean velocity profile U , we solve it and plot the resulting stationary profile. With such an equation, the stationary profile diverges at some finite latitude, that's why we conclude at the end of section 3 that the so called small-scale inertial limit may not be the relevant one from a physical point of view. Realistic values for the parameters of the stochastic forcing and of dissipation taken from data of Jupiter prompt us to consider rather the inertial limit before taking the small-scale forcing limit.

Indeed, we show in section 4 that both limits do commute only for strictly monotonic velocity profiles U . We thus conclude that the appealing formula (1.1) is valid only in some regions of the flow, where U' does not vanish. A more refined analysis is required to deal with the zonal jet velocity extrema, which is the subject of section 4.

In section 4, using Laplace transform tools, we are able to derive an equation for the Reynolds stress divergence in the inertial limit. Taking afterwards the small-scale forcing limit, we give a set of equations that describes the zonal velocity extremum of the eastward jet. Although the full numerical calculation of the solution is avoided, we give some arguments to show that this set of equations leads to the formation of a “cusp” of typical size $\frac{1}{K}$ where $\frac{1}{K}$ is a typical scale of the stochastic forcing. We explain that this cusp has no universal shape, it depends on the spectrum of the stochastic forcing and on the dissipative mechanism, and yet we found a universal relation, valid when viscous phenomena are negligible at the size of the cusp, that relates the curvature of the cusp to the maximal velocity $U(y_{cr})$. It writes (equation (4.6))

$$U(y_{cr})U''(y_{cr}) = -\frac{\epsilon K^2}{r},$$

where r is the linear friction coefficient in s^{-1} . As for the formula (1.1), only the energy injection rate ϵ together with the typical scale of the forcing $\frac{1}{K}$ and the linear friction coefficient r matter, but not the exact Fourier spectrum of the forcing.

On the contrary, the westward jet cannot form this cusp because it would violate the Rayleigh-Kuo criterion of stability. In the last part of this paper (section 4.4.3), we explain how an instability can develop at the extremum of a westward jet, and how this instability stops the growth of the westward jet such that the zonal flow form a parabolic profile of curvature about β .

2. Reynolds stresses from energy, enstrophy, and pseudomomentum balances

2.1. Averaged equations

We start from the equations for a barotropic flow on a periodic beta plane with stochastic forces

$$\begin{aligned} \partial_t V + V \cdot \nabla V &= -rV - \frac{1}{\rho} \nabla P + \beta_d y \begin{pmatrix} V_y \\ -V_x \end{pmatrix} + \sqrt{2\epsilon} f \\ \nabla V &= 0 \end{aligned} \quad (2.1)$$

where $V := \begin{pmatrix} V_x \\ V_y \end{pmatrix}$ is the two dimensional velocity field, r models a linear friction, and f is a stochastic force, that we assume white in time, i.e $\mathbb{E}[f(r, t)f(r, t')] = \delta(t-t')C_f(r, r')$, and β_d is the Coriolis parameter which comes from the fact that the Coriolis force projected on a plane tangent to the sphere depends on the north-south coordinate y . We choose a normalization for the force correlation C_f , such that ϵ is the rate of energy injection in the flow per unit of mass: ϵ has dimensions $m^2 s^{-3}$. In the following, we will always assume that there is no direct energy injection in the zonal velocity profile, i.e that $\frac{1}{L_x} \int dx f(r, t) = 0$.

The main idea is then to separate the flow V in two parts, $V(r, t) = U(y, t)e_x + \begin{pmatrix} u(r, t) \\ v(r, t) \end{pmatrix}$. The mean velocity $Ue_x = \langle V \rangle$ is defined as the zonal and stochastic average of the velocity field. More precisely, we assume that the mean flow is parallel and we take

$U(y)e_x = \frac{1}{L_x} \int dx \mathbb{E}[V(x, y)]$. In the following, the bracket $\langle \rangle$ will be used for this zonal and stochastic average.

In this paper, we will refer to U indifferently as the *mean flow* or *zonal flow*. Let us emphasize here that our aim is not to determine how the mean velocity profile becomes a parallel shear flow, but we assume that the mean flow has this shape and we want then to study the dynamics of the zonal component. It is an empirical evidence that this is indeed the case for many regimes of the barotropic flow equation, especially when β_d is strong enough. Those regimes are of interest for geophysical applications as illustrated by Jupiter or Saturn (Bouchet *et al.* 2016). We note also that the mean flow is not always zonal, especially for small or vanishing values of β_d (Bouchet & Simonnet 2009).

Using this decomposition and the continuity equation, the equation for the mean velocity U becomes

$$\partial_t U + \partial_y \langle uv \rangle = -rU. \quad (2.2)$$

Equation (2.2) shows that the mean flow is forced by the divergence of the Reynolds stress $\partial_y \langle uv \rangle$. In order to reach an equilibrium, this latter term has to balance the dissipation coming from linear friction.

2.2. Energy balance

Let us write the total energy balance

$$\frac{1}{2} \partial_t \langle V^2 \rangle + \partial_y \left(U \langle uv \rangle + \left\langle v \left(\frac{u^2 + v^2}{2} - \frac{p}{\rho} \right) \right\rangle \right) = -r (U^2 + \langle u^2 + v^2 \rangle) + \epsilon \quad (2.3)$$

For the zonal flow, equation (2.2) gives us the balance

$$\frac{1}{2} \partial_t U^2 + U \partial_y \langle uv \rangle = -rU^2.$$

It is interesting for the physical comprehension to write the term $U \partial_y \langle uv \rangle$ as the sum $\partial_y (U \langle uv \rangle) - \partial_y U \langle uv \rangle$, because it shows the existence of an energy flux for the large scale given by $J = U \langle uv \rangle$. The second term $\partial_y U \langle uv \rangle$ is classically interpreted in the literature as the rate of energy transferred from small scales to the zonal flow. In (Ingersoll *et al.* 1981) for example, the authors estimate the correlation coefficient between $\partial_y U$ and $\langle uv \rangle$. If it is strictly positive, it means that the zonal flow has extracted energy from the fluctuations. This decomposition is not unique, but it is physically relevant, because the term $\partial_y U \langle uv \rangle$ has its exact counterpart $-\partial_y U \langle uv \rangle$ in the energy balance for the fluctuations. The energy balance for the large scales of the flow becomes

$$\frac{1}{2} \partial_t U^2 + \partial_y J = \partial_y U \langle uv \rangle - rU^2. \quad (2.4)$$

Then we can subtract this equation from the total energy balance equation (2.3) to get the energy balance for the fluctuations

$$\frac{1}{2} \partial_t \langle u^2 + v^2 \rangle + \partial_y \left\langle v \left(\frac{u^2 + v^2}{2} - \frac{p}{\rho} \right) \right\rangle = -\partial_y U \langle uv \rangle - r \langle u^2 + v^2 \rangle + \epsilon. \quad (2.5)$$

We find that the energy balance is composed of four terms. The stochastic force injects energy at rate ϵ in the flow, and this energy is for one part dissipated by the term $-r \langle u^2 + v^2 \rangle$ whereas an other part is transferred directly to the zonal flow by the term $-\partial_y U \langle uv \rangle$. The energy flux at small scale is $j = \left\langle v \left(\frac{u^2 + v^2}{2} - \frac{p}{\rho} \right) \right\rangle$, it creates a spatial transfer of energy. If we would heuristically identify the zonal flow with the large scales and the fluctuations with the small scales, the flux $v \left(\frac{u^2 + v^2}{2} \right)$ would be related to the

inverse energy cascade towards the larger scales and the term $-\partial_y U \langle uv \rangle$ as a direct transfer from small scale to large scale through non local interaction in Fourier space. For the nonlinear equations, energy is thus transferred to the zonal flow by two mechanisms, a nonlinear interaction between the fluctuations and a direct interaction of the fluctuations with the zonal flow.

We will now do the following assumption: in the stationary regime, all the energy produced at small scales is *locally* (in space) transferred to the largest scale. It means that we neglect dissipation of the fluctuations $r \langle u^2 + v^2 \rangle$, and we neglect also the energy flux $j = \left\langle v \left(\frac{u^2 + v^2}{2} - \frac{p}{\rho} \right) \right\rangle$ coming from the cubic terms and the pressure term, compared to the direct interaction term $\partial_y U \langle uv \rangle$. With this assumption, we then readily get the equality

$$\epsilon = \langle uv \rangle \partial_y U. \quad (2.6)$$

We also note, that from dimensional analysis, assuming that the Reynolds tensor component $\langle uv \rangle$ depends only from the local energy injection rate and the flow shear, this expression could have been obtained immediately, up to a multiplicative nondimensional constant.

We do this approximation here without any justification, because the conditions for it to be valid is precisely one of the aims of this article. But with this assumption, the momentum equation (2.2) becomes solvable because we have an expression for the Reynolds tensor in terms of the mean velocity profile. Explicitly, we get

$$\partial_y \langle uv \rangle = -\epsilon \frac{U''}{U^2}, \quad (2.7)$$

where we have replaced the y-derivative by ' for clarity. What is attracting on this formula is that we can express the Reynold's stress in terms of the mean velocity profile U and this expression does no longer depends on the details of the stochastic forcing, it is simply represented by the energy injection rate ϵ . Using this formula one could solve the ordinary differential equation describing the stationary velocity profile $rU = \epsilon \frac{U''}{U^2}$.

As a matter of fact, this is illusory to believe that such a simple formula could be valid in the general case. There are many indications of that. For example, if the profile U has extrema, which is the case for jets, the energy transfer to the mean flow $U' \langle uv \rangle$ has to vanish because $U' = 0$, and an expression like (2.7) has no chance to be valid. Moreover, Kaushik, Shrinivasan and Young (Srinivasan & Young 2014) have computed explicitly the Reynolds stress for a linear profile, and they found that the result depends on the anisotropy of the correlation function of the noise. They found that the stress is zero for perfect isotropic forcing, a result that was already known from the work of Ioannou. For all these reasons we can not close the equations using approximation (2.7), we need more input from the equations. The first relevant approximation we can do is the quasilinear approximation, which we will discuss in the next subsection.

2.3. Quasilinear approximation and pseudomomentum balance

The first step to do mathematical treatment of equations (2.1) is to chose length and time scales to make the equations nondimensional. There is not just a single accepted way for writing the non dimensional stochastic β plane equations in the literature. We choose here to set temporal and spatial units such that the mean kinetic energy is 1, and $L_x = 1$ (please see (Bouchet *et al.* 2013) for more details, or (Bouchet *et al.* 2016) page 2-3 for comparison with other common nondimensionalization of the equations). Finally, we eliminate the pressure term by taking the rotational of the first equation of (2.1). The

nondimensional equations are

$$\begin{aligned}\partial_t \Omega + V \cdot \nabla \Omega &= -\alpha \Omega - \beta V_y + \sqrt{2\alpha} \eta \\ \nabla V &= 0,\end{aligned}\tag{2.8}$$

where $\eta = \nabla \wedge f$. Now $\alpha = L\sqrt{r^3/\epsilon}$ is a nondimensional parameter although we will often refer to it as the “friction”. $\beta = \sqrt{r/\epsilon}L^2\beta_d$ is the new nondimensional Coriolis parameter, while β_d is the dimensional one. We note that $\beta = L^2/L_R^2$, where $L_R = (\epsilon/r\beta_d^2)^{1/4}$ is Rhines scale. The zonostrophy index used in many references would be $R_\beta = \beta^{1/10}\epsilon^{1/20}r^{-1/4}$. We find that $\alpha \propto (R_\beta)^{-5}$, which implies that the limit of vanishing α corresponds to the limit of large R_β . The Gaussian stochastic term η is defined through its correlation function $\langle \eta(r, t)\eta(r', t') \rangle = C(r - r')\delta(t - t')$. We assume that C is statistically homogeneous such that it depends only on the difference $r - r'$. As a correlation function, C is a definite positive function and has to satisfy the following properties: let us call $\hat{C}_{k,l}$ the Fourier coefficients of C

$$C(x, y) := \sum_{k,l} \hat{C}_{k,l} e^{ikx + ily}\tag{2.9}$$

and $K^2 = k^2 + l^2$, then the function $\hat{C}_{k,l}$ is real and positive. Moreover, if we assume the symmetry $x \rightarrow -x$ and $y \rightarrow -y$, the function $\hat{C}_{k,l}$ is symmetric wrt $k \rightarrow -k$ and $l \rightarrow -l$. The constrain that the mean kinetic energy is one writes $\frac{1}{2} \iint dk dl \frac{\hat{C}_{k,l}}{K^2} = 1$. From now on, the computations will be done with nondimensional quantities. If we want to write a result in its dimensional formulation, we will reintroduce $[\frac{\epsilon}{r}] = m^2.s^{-2}$ and $[L_x] = m$.

The quasilinear approximation has been used for a very long time to study the behavior of the large scales of flows that are dominated by a large scale component, or in plasma physics. Specifically for the problem of jet formation, such a quasilinear approach is at the core of Stochastic Structural Stability Theory (S3T) first proposed by Farrell, Ioannou (Farrell & Ioannou 2003), for quasi-geostrophic turbulence. More recently, an interpretation in terms of a second order closure (CE2) has also been given (Marston *et al.* 2008), and used to describe the transition from homogeneous large scale flows to zonal jets (Srinivasan & Young 2011). It has been shown that this approximation is self consistent in the limit where α goes to zero in equation (2.1) with some assumption on the profile U (stability, no zero modes) (Bouchet *et al.* 2013). This approximation is also believed to be valid for a larger class of situations. In the following we are precisely interested in the small α regime. We will not develop the full justification of the quasilinear approximation here, the interested reader is referred to (Bouchet *et al.* 2013). Let us simply recall the steps leading to the equations with quasilinear approximation. First, we notice that the strength of the noise is of order $\sqrt{\alpha}$. As fluctuations are sheared and transferred to the largest scales on a time scale of order one, this is a natural hypothesis to expect fluctuations (u, v) to be of the same order. This was proven to be self-consistent in (Bouchet *et al.* 2013). We do the substitution $(u, v) \rightarrow \sqrt{2\alpha}(u, v)$ in equation (2.1). The eddy-eddy interaction terms are of order $\alpha^{\frac{3}{2}}$, and can then be neglected. We are left with the set of equations

$$\partial_t U = -\alpha [\partial_y \langle uv \rangle + U]\tag{2.10}$$

$$\partial_t \omega + U \partial_x \omega + (\beta - U'')v = -\alpha \omega + \eta\tag{2.11}$$

where we have introduced $\omega = \partial_x v - \partial_y u = \Delta \psi$, the vorticity of the fluctuations. Equation (2.10) shows that the typical time scale for the evolution of the mean flow U is $\frac{1}{\alpha}$ which is, following our assumption $\alpha \ll 1$, much larger than the time scale for the evolution

of eddies. Using this time scale separation, we will consider that U is a constant field in the second equation (2.11), and we will always solve $\omega(t)$ for a given U . Therefore, the eddy equation becomes linear because U is considered as a given field. This time-scale separation is observed for example on Jupiter where the typical time of eddies evolution ranges from few days to few weeks whereas significant changes in the mean flow are only detected over decades. (see e.g (Porco *et al.* 2003)).

Let us just precise one point: if we had made the quasilinear approximation at the level of the velocity equation (2.1) and studied the energy balance following the steps of section 2.2, we would have get rid of the term $j = \left\langle v \left(\frac{u^2 + v^2}{2} \right) \right\rangle$ in the fluctuation energy balance equation. However, the part of the flux due to the pressure $\partial_y \left\langle v \frac{p}{\rho} \right\rangle$ would still remain in the fluctuation energy budget. Hence, it is not sufficient to have proved self-consistency of quasilinear approximation for small α because it is only a partial explanation of formulas (2.6-2.7). More physical ingredients are needed.

The quasilinear equations conserve energy and enstrophy as the full Navier-Stokes equations. One of the key relation we will use in this paper comes from the fluctuation enstrophy balance,

$$\frac{1}{2} \partial_t \langle \omega^2 \rangle + (\beta - U'') \langle v\omega \rangle = -\alpha \langle \omega^2 \rangle + \frac{1}{2} C(0).$$

As we assume a time scale separation between the zonal flow and fluctuation dynamics, we are interested in the long time behavior of the latter equation. When the vorticity fluctuations ω reach its stationary distribution, we have the equality

$$\langle v\omega \rangle = \frac{1}{U'' - \beta} \left[\alpha \langle \omega^2 \rangle - \frac{1}{2} C(0) \right]. \quad (2.12)$$

Equation (2.12) will be a key formula for our work. Indeed, using the incompressibility condition, we have the equality $\langle v\omega \rangle = -\partial_y \langle uv \rangle$. One can notice looking at (2.12) that in the absence of dissipation and forcing, we have $\langle v\omega \rangle = 0$. In steady state without dissipation and forcing, waves have no effects on the mean flow. This result is classically known in the literature as the non acceleration theorem (see (Gill 1982) p 537 or (Andrews & McIntyre 1978) for a more complete description). It is then natural to expect that any forcing on the mean flow should come from the nonconservative processes which are here only a linear friction and an enstrophy injection at small scales, but we could have add in the equations a viscous term. Without those processes, the left-hand side of equation (2.11) conserves the pseudomomentum $\int \frac{\langle \omega^2 \rangle}{U'' - \beta}$. If $U'' - \beta$ has constant sign in the flow, the conservation of the pseudomomentum does not allow any instability to occur and the flow is stable. This is called the Rayleigh-Kuo criterion for stability of shear flows. If $U'' - \beta$ vanishes somewhere in the flow, an instability may or may not exist. The fact that $U'' - \beta$ vanishes is a necessary condition for instability, not a sufficient one. In equation (2.12), the right-hand side is not defined where $U'' = \beta$. The denominator is zero but the numerator also vanishes. Indeed, for $U'' = \beta$, equation (2.11) reduces to a free transport of the fluctuations and can be solved directly giving $\alpha \langle \omega^2 \rangle - \frac{1}{2} C(0) = 0$. In general, the Reynolds stress divergence remains finite except perhaps at some particular places in the flow as we will discuss in section 4.4.

This means that the latter equation gives us a way to compute the Reynold stress that forces the mean flow:

- We solve the linear equation (2.11) and compute the stationary distribution *as a function of* U .

• Then we can use this expression to close the first equation (2.10), and discuss possible stationary profile U .

Of course things will not be that easy because the dynamics of ω is given by a partial differential equation, and in the general case there are no reasons why we could find any simple expression. Let us focus on the average $\langle \omega^2 \rangle$. First we can take advantage of the invariance along the x direction by taking the Fourier transform of (2.11) in x . The Fourier transform in y does not provide an obvious simplification as the profile U depends on y . However, we can use the linearity to express the solution as the sum of particular solutions for independent stochastic forcings $\eta_l(y, t)$. Each of these forcing has a correlation function $c_l(y) = e^{ily}$, this means that we have the relation $\mathbb{E}[\eta_l(y, t)\eta_l(y', t)] = e^{il(y-y')}\delta(t-t')$. We take the Fourier transform in x defined by $\omega_k(y) := \frac{1}{L_x} \int dx \omega(x, y) e^{-ikx}$ with k taking the values $\frac{2\pi}{L_x}n$, n is an integer. $\omega_{k,l}(y, t)$ is then defined as the function $\omega_k(y, t)$ that is solution of (2.11) with a stochastic forcing with only one Fourier component (k, l) . We then obtain

$$\langle v\omega \rangle = \frac{1}{U'' - \beta} \sum_{k,l} \frac{\hat{C}_{k,l}}{2} [2\alpha \langle |\omega_{k,l}|^2 \rangle - 1], \quad (2.13)$$

where the positive constants $\hat{C}_{k,l}$ are defined by (2.9). Be careful that in this formula the bracket $\langle |\omega_{k,l}|^2 \rangle$ denotes a stochastic averaging, because the zonal average is already taken into account by the sum over all vector k . The vorticity $\omega_{k,l}(y, t)$ is the solution of the stochastic partial differential equation

$$\partial_t \omega_{k,l} + ikU\omega_{k,l} + ik(\beta - U'')\psi_{k,l} = -\alpha\omega_{k,l} + \eta_l. \quad (2.14)$$

As the reader would have notice, we try to reduce the problem by expressing the solution as the sum of particular problem that we hope to be much simpler. Now we have to find an expression for $\omega_{k,l}$ instead of the full solution ω . We will go one step further and show that the stochastic problem described by the two equations (2.13-2.14) reduces in fact to a *deterministic one*, following (Bouchet *et al.* 2013). Equation (2.14) can be formally written as

$$\partial_t \omega_{k,l} + L_k[\omega_{k,l}] = -\alpha\omega_{k,l} + \eta_l,$$

where

$$L_k[\omega_{k,l}] = ikU\omega_{k,l} + ik(\beta - U'')\psi_{k,l} \quad (2.15)$$

is a linear operator for a given U . Then we use the fact that the noise $\eta_{k,l}$ is white in time and has an exponential correlation function $c_l(y) = e^{ily}$ to express the quantity $\langle |\omega_{k,l}|^2 \rangle$ as

$$\langle |\omega_{k,l}|^2 \rangle = \int_{-\infty}^0 dt e^{2\alpha t} |e^{tL_k}[c_l]|^2. \quad (2.16)$$

This formula should be understood as follows: $e^{tL_k}[c_l]$ is the solution at time t of the *deterministic equation* $\partial_t \omega_d + L_k[\omega_d] = 0$ with initial condition $c_l := y \rightarrow e^{ily}$. The subscript d will mean that we are dealing with the solution of a deterministic equation. The exponential $e^{\alpha t}$ ensures the convergence of this integral. The great advantage to have reduced the stochastic problem to a deterministic one is that we now have to solve an hydrodynamic problem, the propagation of a vorticity fluctuation in a shear flow, a problem for which much has already been done in the literature.

2.3.1. Simplifications in asymptotic regimes

Expression (2.16) is still complicated because to get explicit results, it requires to know the behavior of the solution $e^{tL_k}[c_l]$ up to times of order $\frac{1}{\alpha}$. Two parameters can be

used to further simplify the problem, the vector $\mathbf{k} = (k, l)$ and the damping α . We note $K := |\mathbf{k}|$. In this article, we will be interested both in the regime $K \rightarrow \infty$ and $\alpha \rightarrow 0$. The regime of large \mathbf{k} corresponds to a small scale forcing. It will be the aim of part 2 to do an asymptotic computation in this limit. The behavior at leading order in $\frac{1}{K}$ of $\omega_{k,l}$ gives $2\alpha \langle |\omega_{k,l}|^2 \rangle - 1 = 0$, but $\hat{C}_{k,l}$ grows like $K^2 \rightarrow \infty$. That's why we will have to go to next order.

The limit $\alpha \rightarrow 0$ will be called the inertial limit because the fluctuating field is free to evolve without damping. In fact, this limit will be the most difficult one, because we let the turbulence develop on a longer time. But this limit is also the most interesting from a physical point of view because it corresponds to fully turbulent regimes. A rough estimation of the parameters K and α on Jupiter (assuming of course that our model could be valid to describe the behavior of Jupiter's jets) shows that the relevant regime would be $\alpha \rightarrow 0$ before taking the limit $K \gg 1$. Typically, the transition between both regimes will be set by the ratio between $\frac{U''}{K}$ and α . The result in this last regime where $\alpha \ll \frac{U''}{K}$ will depend on whether the deterministic equation

$$\partial_t \omega_d + ikU\omega_d + ik(\beta - U'')\psi_d = 0 \quad (2.17)$$

sustains neutral modes or not. A neutral mode is defined as a solution of this equation of the form $\omega(y, t) = \xi^a(y)e^{ic_a t}$ where c_a is a real constant. It is also sometimes called “modified Rossby waves” in this context, when the jet velocity is nonzero. Two cases can be encountered:

Without modes: Bouchet and Morita (Bouchet & Morita 2010) have shown that without neutral modes, the solution ω_d behaves for long time $\omega_d(y, t) \underset{t \rightarrow \infty}{\sim} \omega_d^\infty(y)e^{ikUt}$, even for non monotonous velocity profiles U . Moreover they give a method to compute this ω_d^∞ using Laplace transform tools. In this case the correlation $\langle v\omega \rangle$ writes in the limit $\alpha \rightarrow 0$

$$\langle v\omega \rangle = \frac{1}{U'' - \beta} \sum_{k,l} \frac{\hat{C}_{k,l}}{2} [|\omega_d^\infty|^2 - 1]. \quad (2.18)$$

We give the full justification of this result in appendix A. From the justification, an interesting remark can be made: when α becomes small, the enstrophy term $\langle \omega^2 \rangle$ diverges as $\frac{1}{\alpha}$, but as the Reynolds stress divergence expression (2.13) involves $\alpha \langle \omega^2 \rangle$, it converges. Such a compensation can be seen as necessary in order to fulfill the pseudomomentum balance.

With neutral modes: We have to modify expression (2.18) to take into account the presence of modes. Again, we leave the technical details to appendice A and we give the final result

$$\langle v\omega \rangle = \frac{1}{U'' - \beta} \sum_{k,l} \frac{\hat{C}_{k,l}}{2} \left[|\tilde{\omega}_d^\infty|^2 - 1 + \sum_{\text{modes } a} |\omega_d^a|^2 \right]. \quad (2.19)$$

This result means that we have to project first the initial condition c_l over the modes labeled by a . The component over the a mode gives the term $\omega_d^a(y)$. This new terms are related to the wave pseudomomentum balance. Then we compute the asymptotic solution $\tilde{\omega}_d^\infty$ of (2.17) using as the initial condition not c_l but $c_l - \sum \omega_d^a$. Briefly speaking, a first reason why there are no cross terms of the form $\omega^a \tilde{\omega}$ between modes and the remaining part of the spectrum is because the frequencies c_a of the modes are always outside of the range of U . The cross terms have an oscillatory part of frequency $\frac{1}{\alpha}(c_a - U)$ that gives a vanishing contribution in the small α limit. This is also related to the fact that, whenever

U is monotonous, the linear operator L_k (2.15) is a normal operator in the norm defined by the pseudomomentum.

Both formulas (2.18-2.19) will be used to study the inertial limit in section 4.

3. The regime of dissipative small scale forcing

3.1. Reynolds stress divergence as a function of U , α and the force correlation function

3.1.1. Reynolds stress divergence as a function of U with finite friction

This section is devoted to the computation of the Reynold's stress divergence $\langle v\omega \rangle$ using equation (2.13), in the limit of small scale forcing i.e $K \rightarrow \infty$. As we consider this limit with fixed α , the flows described by this regime will be characterized by a strong friction strong at the forcing scale. We will consider the case of an infinite space in the y direction, but we expect the result to be qualitatively similar for a finite space because it is sufficient that the scale of the forcing $\frac{1}{K}$ is small compared to the domain size, $\frac{1}{K} \ll L_y$. As was explained in the first part, we have to find the long time behavior of the solution of the deterministic equation (2.17), with the assumption that $K \gg 1$. Please be careful here that K and k are different, $K^2 = k^2 + l^2$. We consider the limit K infinite with both k and l going to infinity such that $l = k \tan \theta$ with θ a fixed constant. We will check that the limit $K \rightarrow \infty$ and $k \rightarrow \infty$ are not at all equivalent. As the leading order term in equation (2.17) is the free transport term $ikU\omega$, we will use the natural Ansatz $\omega_d(y, t) = A_{k,l}(y, t)e^{ikU(y)t}$ in equation (2.17). We obtain for $A_{k,l}$ the equation

$$\partial_t A_{k,l} = -i \frac{U'' - \beta}{k} \int dY H_0(Y) A_{k,l} \left(y - \frac{Y}{k}, t \right) e^{ik(U(y) - U(y - \frac{Y}{k}))t},$$

where H_0 is the Green function of the Laplacian operator $\left(\frac{\partial^2}{\partial y^2} - 1 \right)$, it solves $\left(\frac{\partial^2}{\partial y^2} - 1 \right) H_0(y) = \delta(y)$. The Green function for the full Laplacian $\left(\frac{\partial^2}{\partial y^2} - k^2 \right)$ writes $H_k(y) = \frac{1}{2|k|} H_0(|ky|)$. For infinite space, we have thus $H_0(y) = \frac{1}{2} e^{-|y|}$. This expression is very convenient to do asymptotic calculations because, as the reader can see, $\partial_t A_{k,l}$ is of order $\frac{1}{k}$ and thus goes to zero for large k . At zero order, we have only free transport of the perturbation, and the expression of ω is given by $\omega(y, t) = \omega(y, 0)e^{ikU(y)t}$. The computation of the next order is rather technical, and is developed in appendix B. It happens that we can compute not only the divergence of the Reynolds stress, but we can integrate the result to obtain even the Reynolds stress itself. We let $\tan \theta = \frac{l}{k}$ be the ratio between the y wise and x wise forcing scales. We first do the computation for a single finite value of the parameter θ (for non zero k). The result is

$$\mathcal{R}e \langle u_\theta v_\theta^* \rangle = \frac{\hat{C}_{k,l}}{4k^2} \text{Im} \int_{-\infty}^{+\infty} \frac{Y e^{-|Y|} e^{-iY \tan \theta}}{(2\alpha - iU'(y)Y)} dY. \quad (3.1)$$

Let us comment on this result. The parameter α is small because we have done the quasilinear approximation, but we keep it finite. It has a regularizing effect, and ensures that the integral remains well defined for every profile U even if $U' = 0$ somewhere in the flow. The result above does not really makes sense for θ close to $\frac{\pi}{2}$ because it was assumed from the beginning that the value $\frac{\pi}{2}$ is excluded. In numerical simulations, the spectrum of the stochastic forcing is often an annulus with a weight function to make it more or less anisotropic. The Fourier component $k = 0$ is excluded because it corresponds to a direct stochastic forcing on the zonal flow (see figure (1)). To get results we can compare to simulations, we have to integrate the contributions to the Reynolds stress over the whole spectrum.

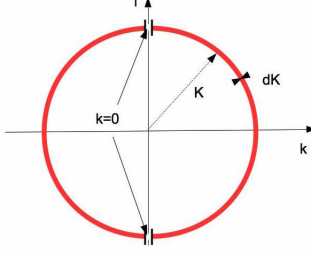


FIGURE 1. Typical spectrum of the stochastic forcing

We will thus define a weight function $\hat{g}(\tan \theta)$ such that the correlation function Fourier component is $\hat{C}_{k',l'} = \hat{g}(\tan \theta) K \delta(K' - K)$. In figure (1) for example, we have a constant function \hat{g} except around the excluded values $\frac{\pi}{2}$ and $-\frac{\pi}{2}$. We approximate the discrete sum in (2.13) by an integral assuming $\frac{1}{L_x} \ll dK$. Because we have fixed the mean kinetic energy to 1, the function \hat{g} must satisfy

$$\frac{1}{2} \iint dk' dl' \frac{\hat{C}_{k',l'}}{K'^2} = \frac{1}{2} \iint K' dK' d\theta \frac{\hat{g}(\tan \theta) K \delta(K' - K)}{K'^2} = \int_{-\infty}^{+\infty} dx \frac{\hat{g}(x)}{1+x^2} = 1,$$

In the last integral, we have done the change of variable $\tan \theta = x$. Using this function to characterize the spectrum, we obtain the simple expression for the Reynolds stress

$$\langle uv \rangle(y) = \pi \text{Im} \int_{-\infty}^{+\infty} \frac{Y e^{-|Y|} g(-Y)}{(2\alpha - iU'(y)Y)} dY, \quad (3.2)$$

where g is the inverse Fourier transform of \hat{g} , $g(Y) = \frac{1}{2\pi} \int dx \hat{g}(x) e^{iYx}$. Now that we have an expression for the Reynolds stress in terms of the mean profile U we can solve equation (2.2) and find the stationary solution, if any. This work will be done in the subsection 3.2, where we will use the above formula.

Let us conclude this section with a comparison between this result and the one obtained in (Srinivasan & Young 2014) in case of a linear profile $U(y) = \gamma y$. For an isotropic forcing, i.e for constant \hat{g} , the function g is proportional to the delta function. The Reynolds stress is then zero. On the contrary, take \hat{g} to be a delta function $\delta(x)$, the function g is constant and we find

$$\langle uv \rangle(y) = \int_0^{+\infty} \frac{U' s^2 e^{-s}}{(4\alpha^2 + U'^2 s^2)} ds, \quad (3.3)$$

which corresponds to the exact expression computed by Kaushik, Srinivasan and Young in case of a fully anisotropic forcing. Therefore we conclude that our result are physically consistent. For the linear profile, the *exact* expression given in (Srinivasan & Young 2014) for the Reynolds stress is

$$U' \langle uv \rangle_\theta = 1 - \int_0^{+\infty} dt e^{-t} \frac{1 + \tan^2 \theta}{1 + (\tan \theta - \frac{U'}{2\alpha} t)^2}. \quad (3.4)$$

We find the result $U' \langle uv \rangle_\theta \rightarrow 1$ when α becomes small, which coincides with the formula (2.6) obtained by neglecting some of the terms in the energy balance, and thus justifying it for this case. However expression (3.4) coincides with (3.3) in the limit where $\theta = 0$ only. To compute an exact expression like (3.4), one has to use another method detailed in (Srinivasan & Young 2014) without using our approximations of small-scale forcing.

3.1.2. Reynolds stress divergence as a function of U in the limit of small friction

Having found the general formula for the Reynolds stress (3.2), we can consider the limit $\alpha \rightarrow 0$. In this limit the Reynolds stress is no longer defined everywhere because the limit $\alpha \rightarrow 0$ is defined only when U' is nonzero. However, equation (3.2) tells us that the limit of $U' \langle uv \rangle$ is always defined, even for $U' = 0$. It writes

$$U' \langle uv \rangle(y) \xrightarrow{\alpha \rightarrow 0} \pi \int_{-\infty}^{+\infty} e^{-|Y|} g(-Y) dY.$$

We transform this expression using the Fourier transform of $e^{-|Y|}$ and g , noting that $2\pi \int_{-\infty}^{+\infty} e^{-|Y|} g(-Y) dY = \int_{-\infty}^{+\infty} dx \frac{2}{1+x^2} \hat{g}(x) = 2$. It gives the final result

$$U' \langle uv \rangle \xrightarrow{\alpha \rightarrow 0} 1, \quad (3.5)$$

which writes in its dimensional formulation

$$U' \langle uv \rangle \xrightarrow{r \rightarrow 0} \epsilon,$$

everywhere in the flow. This is our first main result, it is consistent with the result (2.7) we found by studying the energy balance. Nevertheless, this result should be considered with care. It tells us that in the limits $K \rightarrow \infty$, $\alpha \rightarrow 0$ taken in this order, the energy is totally transferred from small scales to large scales. This is physically consistent: with the limit of large K , the eddy evolution becomes local. Everything happens as if the perturbation only sees a region of width $\frac{1}{K}$ around itself, and thus the different parts of the flow are decoupled. The other limit of small α forces the energy to go to the large scale to be dissipated because the dissipation at small scales becomes negligible. Another assumption which is quite hidden in our calculation is the fact that the forcing is not isotropic. If it is, the Reynolds stress is zero, that's what we emphasized on expression (3.2) before we took the limit $\alpha \rightarrow 0$. The case of fully isotropic forcing is also a limit case that is in fact never satisfied in real systems or in numerical systems because there is always small anisotropy coming from discretization of the Fourier spectrum in numerical simulations, or nonlinearities or other physical constraints.

As a conclusion to this section, let us discuss again the energy balance for the fluctuations defined by (2.5). With the quasilinear approximation, it reduces to

$$\frac{1}{2} \partial_t \langle u^2 + v^2 \rangle - \frac{1}{\rho} \partial_y \langle vp \rangle = -U' \langle uv \rangle - r \langle u^2 + v^2 \rangle + \epsilon.$$

The term $\langle pv \rangle$ is quadratic in the fluctuations, that's why it remains in the energy balance. This term is responsible for a possible energy flux at the small scales of the flow. The computation of the pressure requires to invert the Laplacian operator. It is then natural to expect that the pressure has an asymptotic expansion when $K \rightarrow \infty$ with the leading order proportional to $\frac{1}{K^2}$. This explains qualitatively why the energy flux represented by the term $\frac{1}{\rho} \langle pv \rangle$ vanishes in the limit of large K and why the energy transfer becomes purely local in space. In the limit $K \rightarrow \infty$, the quadratic terms $\langle u^2 \rangle$ and $\langle v^2 \rangle$ have finite limits, and the linear dissipation $r \langle u^2 + v^2 \rangle$ contributes to the energy balance. Hence $U' \langle uv \rangle \neq \epsilon$. After we take the limit $r \rightarrow 0$, the only way to dissipate the fluctuation energy is to transfer it to the mean flow by the term $U' \langle uv \rangle$, and this gives the equality $U' \langle uv \rangle = \epsilon$.

3.2. Self consistent jet profile

We are now discussing the possibility to have a stationary profile U in the dissipative small scale forcing regime. We first do not consider the limit $\alpha \rightarrow 0$. We have a closed set

of equations from (2.10) and (3.2), that we will rewrite this way: we let χ be the function defined through $\chi(x) := \pi \text{Im} \int_{-\infty}^{+\infty} \frac{Y e^{-|Y|} g(-Y)}{(1-ixY)} dY$, and the stationary profile is defined by the set

$$\begin{aligned} \partial_y \langle uv \rangle &= -U \\ \langle uv \rangle &= \frac{1}{2\alpha} \chi \left(\frac{U'}{2\alpha} \right). \end{aligned}$$

The beautiful fact is that this system is integrable. If we replace $\langle uv \rangle$ in the first equation, it comes

$$\frac{U''}{2\alpha} \frac{1}{2\alpha} \chi' \left(\frac{U'}{2\alpha} \right) = -U, \quad (3.6)$$

so we can now multiply the equality by U' and integrate. Let X be a primitive of $x\chi'(x)$ and C the integration constant, we have

$$X \left(\frac{U'}{2\alpha} \right) + \frac{1}{2} U^2 = C. \quad (3.7)$$

In general, X does not seem to have any simple analytical expression, but as we have explicit formula for its derivative, we can easily study the behavior of the dynamical system described by equation (3.7). As an alternative point of view, let us notice that equation (3.7) can be expressed as the extrema of some functional of U

$$\begin{aligned} \frac{\delta I}{\delta U} &= 0 \\ I[U] &= \frac{1}{2} U^2 - \Gamma \left(\frac{U'}{2\alpha} \right) \end{aligned}$$

where Γ is a primitive of the function χ . In our problem, $I[U]$ is a kind of energy functional for the system, and one can interpret the term $\Gamma \left(\frac{U'}{2\alpha} \right)$ as a potential energy.

The extrema of X are given by the equation $x\chi'(x) = 0$. X is an even function which implies for the velocity profile U that the increasing and decreasing parts of the profile are symmetric. We are then looking for the zeros of $\chi'(x) = \int f(Y) \frac{Y^2(1-x^2Y^2)}{(1+x^2Y^2)^2} dY$, where we have set $f(Y) := \pi e^{-|Y|} g(-Y)$. χ' is even. We know that f is a positive integrable symmetric function and its integral is 1. We immediately see that $\chi'(0) > 0$, and an asymptotic calculation shows that $\chi'(x) \sim -\frac{1}{x^2}$ at infinity. Therefore, the function χ' has at least two zeros, symmetrically localized around 0, γ and $-\gamma$ say. Moreover if the function f has a monotonic behavior, one can show that these are the only zeros of χ' . Therefore, for monotonic f the potential X has 3 extrema, and there exists a well in the potential between $-\gamma$ and γ . One example of such functions χ' and X is given in figure (2).

For non monotonic or more eccentric functions f , we can have more extrema for X , but a small study of the behavior of X around zero will show that 0 is always a local minimum for X . We conclude that the potential has at least one well at zero whatever the function f and that a periodic solution to (3.7) always exists.

We have depending on the value of the constant in (3.7) periodic solutions or diverging solutions. All these properties are illustrated in the figures (4).

In equation (3.7), X plays the role of a potential, and the dynamics is similar to a particle moving in a potential. The only difference is that the roles of U and U' are exchanged compared to the role of x and \dot{x} for a particle in a potential. The constant in the right-hand side is set by $U'(0)$ because $C = X \left(\frac{U'(0)}{2\alpha} \right)$. Depending on the value

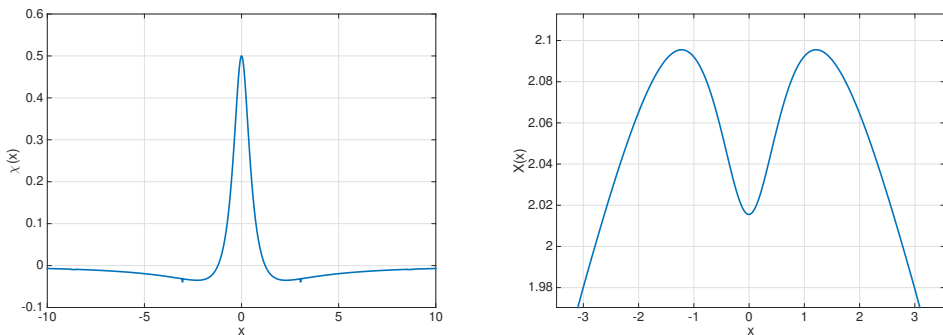


FIGURE 2. The functions χ' (left) and X (right) when f is a normal Gaussian function. The function χ' is symmetric with two zeros, and X has three extrema. The potential X has a well which means that periodic solutions can exist.

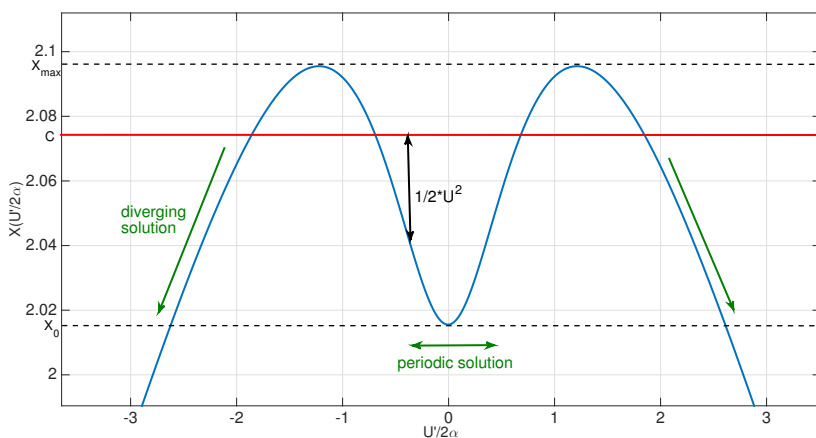


FIGURE 3. In the limit of small scale forcing, the mean flow can be computed analytically from the Newtonian Eq. (3.7). We show here that the situation is analogous to a particle moving in a one-dimensional potential. The curve displays the potential X appearing in Eq.(3.7). If the constant C is between X_0 and X_{max} as is the case in the figure, there are three solutions allowed. Two of them have a divergent velocity field U , but one is periodic and bounded by $U_{max} = \sqrt{2C - X_0}$. For other values of C outside the range $X_0 - X_{max}$, the periodic solution disappears.

of this constant, there can be one, two or three solutions. The situation is represented in figure (3). If $C > X_{max}$, there is one solution for which U never vanishes. If $X_0 < C < X_{max}$, there are three possible solutions, one is periodic, the two other diverge. The periodic solution corresponds to $\frac{U'}{2\alpha}$ confined in the well of X . In that case the flow is periodic and the solution exchanges kinetic energy in the term $\frac{1}{2}U^2$ with potential energy $X\left(\frac{U'}{2\alpha}\right)$. This situation is analogous to a particle moving in a potential. Outside the well, the solutions are diverging, one corresponds to an increasing U and the other to a decreasing U . If finally $C < X_0$ only diverging solutions remain possible.

Our model predicts both divergent or periodic stationary profiles depending on the value of the constant in (3.7). The transition between the two regimes is governed by the parameter $\frac{U'(0)}{2\alpha}$. If $\frac{U'(0)}{2\alpha}$ is in the interval $[-\gamma, \gamma]$, then the solution is confined in the

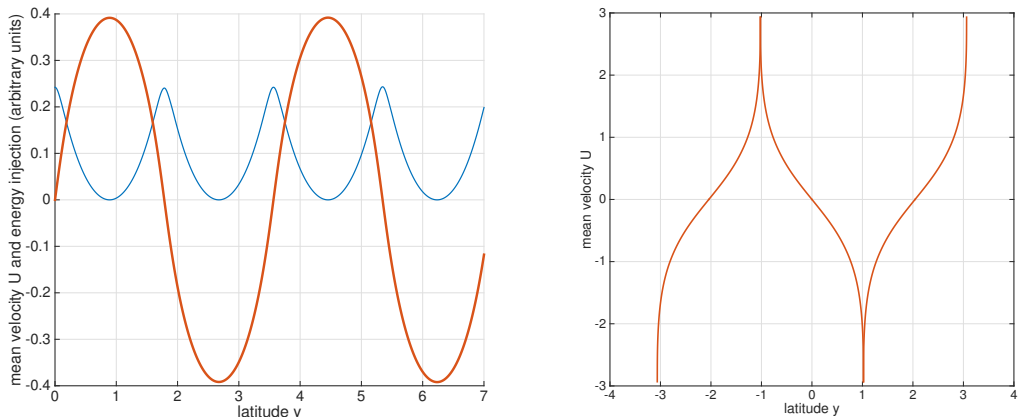


FIGURE 4. Mean velocity profile U , when f is a normal Gaussian function. With $U'(0) = 1$ and $\alpha = 0.5$ we obtain a periodic profile (left picture). The thin curve is the energy transfer $U' \langle uv \rangle$. With $U'(0) = 1$ and $\alpha = 0.1$ we obtain a succession of divergent profiles (right picture). On the picture, the velocity profile has been obtained by plotting together diverging solutions.

well of the potential and is therefore periodic and regular. The numerical estimation of γ is $\gamma \simeq 1, 22$ for $f(Y) = \frac{1}{\sqrt{\pi}} e^{-Y^2}$. To obtain regular periodic profiles, one has to keep $\frac{U'_0}{2\alpha}$ between $-\gamma$ and γ , and if α goes to zero, U'_0 has to vanish too. When α goes to zero the periodicity of this type of profiles becomes infinite, growing like $\frac{1}{\alpha}$. α gives a spatial scaling of the solution. Define $\tilde{U}(y) = U\left(\frac{y}{2\alpha}\right)$, then \tilde{U} satisfies the equation

$$X(\tilde{U}') + \frac{1}{2}\tilde{U}^2 = C.$$

Therefore, changing the parameter α is the same as doing a rescaling in y . If the solution of the latter equation is periodic of period L , the solution U will be periodic of period $\frac{L}{2\alpha}$.

A relevant question is the stability of such profiles. We will try to give a qualitative argument to explain why a periodic profile like the one on the left of figure (4) is unstable for the dynamics

$$\partial_t U = -\frac{U''}{4\alpha^2} \chi' \left(\frac{U'}{2\alpha} \right) - U. \quad (3.8)$$

We will call U_0 the stationary *periodic* profile and study the linearized dynamics of (3.8) around U_0 . Injecting $U_0 + \delta U$ in the equation and keeping only the linear terms in δU gives

$$\delta \dot{U} = -\frac{1}{4\alpha^2} \chi' \left(\frac{U'_0}{2\alpha} \right) \delta U'' - \frac{U_0''}{4\alpha^2} \chi'' \left(\frac{U'_0}{2\alpha} \right) \frac{\delta U'}{2\alpha} - \delta U.$$

This equation has the general form

$$\delta \dot{U} = -a_2(y) \delta U'' - a_1(y) \delta U' - \delta U,$$

where a_1, a_2 are some functions depending on the stationary solution $U_0(y)$. The behavior of the solution results on the effect of three terms: the term in $\delta U''$ is a diffusive term, the term in $\delta U'$ makes the solution propagate on the y axis, and the last term is a linear damping. For the question of stability, the sign of the diffusion coefficient $-a_2$ in front of $\delta U''$ will be crucial. We see that the sign of a_2 is the same as for $\chi' \left(\frac{U'_0}{2\alpha} \right)$. For the periodic

solution in the left of figure (4), $\chi' \left(\frac{U'_0}{2\alpha} \right)$ is always strictly positive. Therefore the periodic solution corresponds to a *negative* diffusion coefficient, which makes the equation very unstable for large wavenumbers. On the contrary, the diverging solution on the right of figure (4) corresponds to $\chi' \left(\frac{U'_0}{2\alpha} \right)$ always strictly negative and thus a strictly *positive* diffusion coefficient. We expect the divergent profile to be stable for the dynamics defined by (3.8).

Let us summarize what we found in this section. We studied the limit $K \rightarrow \infty$ for the quasilinear dynamics of fluctuations. We found that the Reynolds stress divergence can be expressed in terms of the zonal flow U and its derivatives, which allow to write a *closed* PDE for the dynamics of U . We solved the stationary equation for U and found that two solutions can exist when α is finite. One solution is regular and periodic, the other one has singularities, it is the juxtaposition of divergent profiles. (see figure (4)). With a qualitative argument, we explained why the stable solution should be the singular one. For a real flow, such a divergence cannot occur. The fact that Eq. (3.7) predicts diverging profiles U shows that the expression for the Reynolds stress (1.1) is not valid everywhere in the flow, but it holds only in the spatial subdomains where the flow is monotonic, not at the extrema. If K is finite, there should be a regularizing mechanism at scale $\frac{1}{K}$ that stops the growth of the mean velocity profile and regularizes the solution U at scale $\frac{1}{K}$. “Cusps” of typical size $\frac{1}{K}$ should be created at places where the solution U is diverging. However, this is only one part of the mechanism. On Jupiter as well as in numerical simulations, cusps can be observed only for the eastward part of the flow. (see figure (8)) For the westward part, the flow is more parabolic with a curvature close to β . In section 4.4, we will try to answer the question why a cusp cannot occur for westward jets. Let us now precise that a cusp for a westward jet violates the Rayleigh-Kuo criterion for stability whereas a cusp on eastward jets does not. The mechanism for the formation of a parabolic profile is the hydrodynamic instability.

4. Inertial small scale forcing regime

In section 3, we took the limit $K \rightarrow \infty$ before $\alpha \rightarrow 0$, which means physically that we were assuming $\frac{U''}{K\alpha} \ll 1$ in the flow. Looking at Jupiter, one could wonder if this regime is the relevant one. Observations collected by the probes Gallileo, Cassini (see (Porco *et al.* 2003) and others) allows to estimate typical values of K and α . K can be estimated with the typical size of cyclones in Jupiter’s atmosphere, which are typically of 1000 km. The dissipation on Jupiter involves different mechanisms, which are all “hidden” in the linear friction. It is not at all obvious what could be a typical time scale for dissipation. We consider a time of 1500 days. The data provide us an estimation of U_{rms} , and the Coriolis parameter β is easily computed from the rotation rate of Jupiter. It is convenient to chose a spatial scaling such that the typical length of a jet is one, and -as was done in equation (2.8)- to scale the mean velocity U_{rms} to one. With this particular scaling, we would have $K \sim 0.1$ and $\alpha \sim 10^{-3}$. The typical length for a jet is of order 1 and therefore U'' should also be of order 1. To model the flow on Jupiter, we have to take rather $\alpha \rightarrow 0$ first, it will be relevant whenever $\frac{U''}{K\alpha} \gg 1$.

Nothing tells us a priori that the limits in K and α commute. This question is the subject of the present section. Please take note that we are always dealing with the deterministic problem of time evolution of a perturbation (2.17) and we will stop using the subscript d for the deterministic solution ω_d . This deterministic problem with $\frac{U''}{K\alpha} \gg 1$ is much more difficult to analyze.

4.1. Computation of ω^∞

In the following and until section 4.4, we assume there are no Rossby waves in the flow. It has been shown long ago that those waves travel at a velocity $c < U_{min}$ (Drazin *et al.* 1982; Pedlosky 1964). In case of jets, this property imply that they are localized around the extrema of westward jets. We do not know any method to compute those waves for a general mean flow U . In section 4.4, we will explain how we can compute them in case of a parabolic profile. It will be shown that the waves exist only for a curvature $0 < U'' < \beta$ and that there is at least one Rossby wave in this configuration. In particular, when $U'' < 0$ as for the cusp of westward jets, we expect no waves, that's why this case is of interest and we postpone their computation to section 4.4.

In this subsection, we will summarize the main result obtained by Bouchet and Morita (Bouchet & Morita 2010) that allows us to compute the function $\omega_{k,l}^\infty$ that appears in (2.18). $\omega_{k,l}^\infty$ gives then an easy access to the small α limit, independently of the large K limit.

We start from equation (2.17) that describe the linear evolution of a perturbation $\omega(y, t)e^{ikx}$ of meridional wave number k , and with streamfunction $\psi(y, t)e^{ikx}$. The idea is to transform equation (2.17) into an inhomogeneous Rayleigh equation, as classically done, and then to study its asymptotics solutions close to the real axis, which is the limit $\epsilon \rightarrow 0$, with the notations below. We introduce the function $\varphi_\epsilon(y, c)$ which is the Laplace transform of the stream function $\psi(y, t)$ i.e $\varphi_\epsilon(c) := \int_0^\infty dt \psi(y, t) e^{-ik(c+i\epsilon)t}$. To avoid any confusion, we stress that in this section, ϵ will always denote in this section a small parameter and not the energy injection rate. The Laplace transform φ_ϵ is well defined for any non zero value of the real variable ϵ with a strictly negative product $k\epsilon$. c has to be understood as the phase speed of the wave, and $k\epsilon$ is the (negative) exponential growth rate of the wave. We will set the energy injection to 1. Using the same notations as in (Bouchet & Morita 2010), the equation for φ_ϵ is

$$\left(\frac{d^2}{dy^2} - k^2 \right) \varphi_\epsilon(y, c) + \frac{\beta - U''(y)}{U(y) - c - i\epsilon} \varphi_\epsilon(y, c) = \frac{\omega(y, 0)}{ik(U(y) - c - i\epsilon)}, \quad (4.1)$$

with the boundary conditions that φ_ϵ vanishes at infinity. We do not have a flow infinite in the y direction, but as was already stated, the properties of the flow become local for large K . The choice to take vanishing boundary conditions at infinity is done for convenience and it is expected that this particular choice does not modify the physical behavior of the perturbation.

For all $\epsilon > 0$ the function φ_ϵ is well defined. The inhomogeneous Rayleigh equation (4.1) is singular for $\epsilon = 0$ and any critical point (or critical layer) y_c such that the zonal flow velocity is equal to the phase speed: $U(y_c) = c$. One can show that φ_ϵ has a limit denoted φ_+ when ϵ goes to zero. The function ω^∞ is then given by

$$\omega^\infty(y) = ik(U''(y) - \beta)\varphi_+(y, U(y)) + \omega(y, 0), \quad (4.2)$$

see (Bouchet & Morita 2010). The function ω^∞ depends on the Laplace transform of the stream function but for a phase velocity c equal to the zonal velocity at latitude y . From a mathematical point of view, it corresponds to the value of φ_+ exactly at its singularity. The singularity in equation (4.1) is of degree one (proportional to $\frac{1}{y}$) except at the extrema of the jets where it is of degree two. A singularity of order two would create a divergence for the solution, but it happens that the numerator in (4.1) vanishes at such points and the solution is still defined at the extrema of a jet. A nontrivial consequence of that is

$$\omega^\infty(y_c) = 0$$

at all critical latitudes y_{cr} where $U' = 0$. This result, called depletion of vorticity fluctuation at the jet critical points in (Bouchet & Morita 2010), has important physical consequences that influence the dynamics of a jet.

As described in (Bouchet & Morita 2010), using formula (4.1) and (4.2), one can numerically compute the function ω^∞ : we first have to solve a set of boundary value problems for ordinary differential equations parameterized by c and ϵ to obtain a solution family $\varphi_\epsilon(c)$. Then we evaluate, for small enough ϵ each solution $\varphi_\epsilon(c)$ at the value y_c satisfying $U(y_c) = c$. This method is much faster and has less numerical cost than computing the long time evolution of the partial differential equation (2.17). We use this method in the following of this section.

4.2. Limit of small scale forcing for monotonic profiles

Again, we assume there are no Rossby waves. We will now consider the limit of small scale forcing. The question is: do we find the results of section 3 when taking the limit $\alpha \rightarrow 0$ before the limit $K \rightarrow \infty$? This question is crucial and not easily answered. The calculations are rather technical and can be skipped in the first lecture. We will prove that the limits do commute only for strictly monotonic profiles. If U' never vanishes, we will find again the result of section 3 where we found that $\langle v\omega \rangle \underset{K \rightarrow \infty}{\sim} -\frac{U''}{U'^2}$ in the limit $\alpha \rightarrow 0$. (recall that the mean kinetic energy is set to one)

We start from equation (4.1) that describes the inertial behavior of a deterministic evolution of a perturbation $\omega(y, 0)$ when ϵ vanishes. Using the Green function $H_k(y)$ of $(\partial_y^2 - k^2)$ we write

$$\varphi_\epsilon(y, c) = (U''(y) - \beta) \int dy' H_k(y') \frac{\varphi_\epsilon(y - y', c)}{U(y - y') - c - i\epsilon} + \int dy' H_k(y') \frac{\omega(y - y', 0)}{ik(U(y - y') - c - i\epsilon)}.$$

Now we make the change of variable $Y = ky'$. The Green function has the scaling $H_k(y') := -\frac{1}{2k} H_0(Y)$. Recalling that $\varphi_+(y, c) = \lim_{\epsilon \downarrow 0} \varphi_\epsilon(y, c)$, it follows

$$\begin{aligned} \varphi_+(y, c) = & -\frac{(U''(y) - \beta)}{2k^2} \lim_{\epsilon \rightarrow 0} \int dY H_0(Y) \frac{\varphi_\epsilon(y - \frac{Y}{k}, c)}{U(y - \frac{Y}{k}) - c - i\epsilon} \\ & - \frac{1}{2ik^3} \lim_{\epsilon \rightarrow 0} \int dY H_0(Y) \frac{\omega(y - \frac{Y}{k}, 0)}{U(y - \frac{Y}{k}) - c - i\epsilon}. \end{aligned} \quad (4.3)$$

Please note that we are again making the assumption that $\frac{l}{k} := \tan \theta$ is finite and thus $K \rightarrow \infty$ implies $k \rightarrow \infty$. Let us remind here that it is crucial to take the limit $\epsilon \rightarrow 0$ first before $K \rightarrow \infty$ because ϵ plays exactly the role of the linear friction in section (3). If we want to study the inertial regime, we have to take a vanishing friction first. In (Bouchet & Morita 2010), it is shown that the function φ_ϵ has the finite limit φ_+ .

Consider now the magnitude of both terms in the right-hand side of (4.3). We have a term depending on φ_+ and another depending on the initial condition $\omega(y, 0)$. The initial condition is of order 1, and then the second term will be of order $\frac{1}{k^3}$. As a consequence, the first term in the asymptotic expansion of φ_+ will be of order $\frac{1}{k^3}$. The first term in the right-hand side of (4.3) gives the next order of the asymptotic expansion and is thus negligible. We write

$$\varphi_+(y, c) \underset{K \rightarrow \infty}{\sim} -\frac{1}{2ik^3} \lim_{\epsilon \rightarrow 0} \int dY H_0(Y) \frac{\omega(y - \frac{Y}{k}, 0)}{U(y - \frac{Y}{k}) - c - i\epsilon}. \quad (4.4)$$

Combining equations (4.2) and (4.4) we find that

$$|\omega^\infty(y)|^2 \underset{K \rightarrow \infty}{\sim} |\omega(y, 0)|^2 - \frac{U'' - \beta}{k^2} \mathcal{R}e \left\{ \lim_{\epsilon \rightarrow 0} \int dY H_0(Y) \frac{\omega * (y, 0) \omega(y - \frac{Y}{k}, 0)}{U(y - \frac{Y}{k}) - U(y) - i\epsilon} \right\}.$$

The final step is to replace $\omega(y, 0) = e^{ily}$, and $H_0(Y) = e^{-|Y|}$. We use also the Sokhotski–Plemelj formula: $\lim_{\epsilon \rightarrow 0} \frac{1}{x - i\epsilon} = i\pi \delta(x) + \mathcal{P} \left(\frac{1}{x} \right)$, to obtain

$$\begin{aligned} |\omega^\infty(y)|^2 \underset{K \rightarrow \infty}{\sim} |\omega(y, 0)|^2 - \frac{U'' - \beta}{k^2} \mathcal{R}e \left\{ \lim_{\epsilon \rightarrow 0} \int dY e^{-|Y|} \frac{e^{-iY \tan \theta}}{U(y - \frac{Y}{k}) - U(y) - i\epsilon} \right\} \\ \underset{K \rightarrow \infty}{\sim} |\omega(y, 0)|^2 - \frac{U'' - \beta}{k^2} \mathcal{R}e \left\{ i\pi \int dY e^{-|Y|} e^{-iY \tan \theta} \delta \left(U \left(y - \frac{Y}{k} \right) - U(y) \right) \right\} \\ - \frac{U'' - \beta}{k^2} \mathcal{R}e \left\{ \mathcal{P} \left\{ \int dY e^{-|Y|} \frac{e^{-iY \tan \theta}}{U(y - \frac{Y}{k}) - U(y)} \right\} \right\} \\ \underset{K \rightarrow \infty}{\sim} |\omega(y, 0)|^2 - \frac{U'' - \beta}{k^2} \mathcal{P} \left\{ \int dY e^{-|Y|} \frac{\cos(Y \tan \theta)}{U(y - \frac{Y}{k}) - U(y)} \right\}, \end{aligned}$$

where we have used that the term $i\pi \int dY e^{-|Y|} e^{-iY \tan \theta} \delta \left(U \left(y - \frac{Y}{k} \right) - U(y) \right)$ is purely imaginary. Injecting this result in (2.18) gives the contribution of one Fourier mode k, l with $\frac{k}{l} = \tan \theta$ to the Reynolds stress divergence

$$\mathcal{R}e \langle v_\theta^* \omega_\theta \rangle \underset{K \rightarrow \infty}{\sim} - \frac{\hat{C}_{k,l}}{2k^2} \mathcal{P} \left\{ \int dY e^{-|Y|} \frac{\cos(Y \tan \theta)}{U(y - \frac{Y}{k}) - U(y)} \right\}.$$

Some lengthy calculations are required to show that this expression coincides with $\frac{U''}{U'^2}$, for an energy injection rate equal to one. We do it in appendix C. But we have to do an additional assumption: the asymptotic expansion is valid only if $\frac{kU'}{U''} \rightarrow \infty$. There should exist a small region in the vicinity of the extremum $U' = 0$ where this calculation breaks down. The formula can be valid only for strictly monotonic profiles or for the monotonic part between two extrema of a jet.

We have shown that the limit of vanishing friction and small scale forcing commute for a strictly monotonic velocity profile U . In these limits, the Reynolds stress does not depend on the shape of the stochastic forcing. It is worth to emphasize that our results are asymptotic results. The behavior may be really different for finite friction and finite K . The work done in (Srinivasan & Young 2014) shows that the shape of the stochastic forcing matters in the general case. Jets have nonmonotonic velocity profile U . In the limit $K \rightarrow \infty$ first, figure (4) shows the existence of a cusp at the extremum of the jet. The extremum is a place where the velocity profile has a structure at scale $\frac{1}{K}$, and therefore $\frac{U''}{K\alpha}$ is large. What is the behavior of a jet in the vicinity of an extremum is the subject of the following sections.

4.3. Cusps for eastward jets

In the previous parts of this paper, we saw that the formula $\langle v\omega \rangle = -\frac{U''}{U'^2}$ gives a divergent mean velocity profile and we discussed that this formula can be valid only in the limit $\frac{kU'}{U''} \rightarrow \infty$. It is thus natural to think that this formula for the divergence of the Reynolds stress is valid between the extrema of the jet, but in a region of size $\frac{1}{K}$ around the extremum, another mechanism should take place to stop the jet growth. On Jupiter, the data collected by Galileo and Cassini probes, shown in figure (5), indicate that the

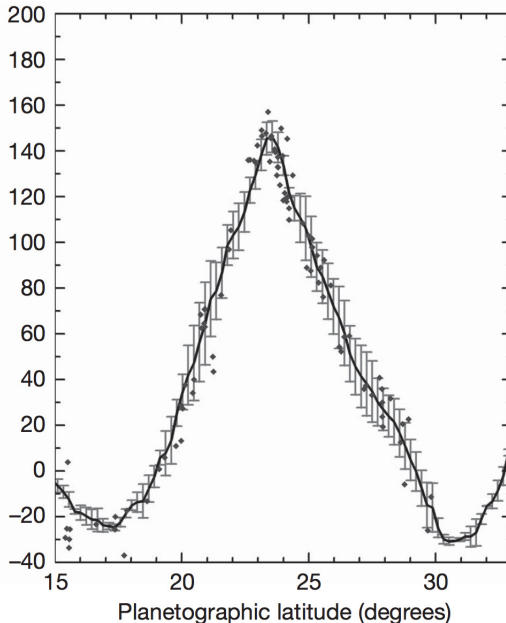


FIGURE 5. The 24°N Jupiter eastward jet (taken from (Sánchez-Lavega *et al.* 2008)). The vertical scale is the mean velocity of the wind ($m.s^{-1}$).

eastward jets have “cusps”, while westward jets seem smoother. We first discuss eastward jet cusps.

Looking more precisely on these cusps in figure (5), we see that their size is approximately 1 degree i.e a scale of ~ 1000 km. When we observe the surface of the planet, we can see the fluctuating vortices evolving in a timescale of few days. The size of those vortices are related to three dimensional motions, producing convection plumes, that develop potential vorticity disturbances at a scale which approximately the Rossby deformation radius of order 1,000 km and with potential vorticity of order β , the Coriolis parameter. In our effective model of a barotropic flow, those convective phenomena are modeled by the stochastic force, and this gives us a rough estimate of the scale $\frac{1}{K}$, of order of a thousand kilometers. Those observations are consistent with our finding that the cusp should be regularized at a scaled of order $1/K$.

Our question is: can we have a cusp solution of the stationary equation

$$\langle v\omega \rangle [U] = U,$$

in the limit $K \rightarrow \infty$?

The idea is to take equation (4.1) and study its large asymptotic after changing the scale $y \leftarrow Ky$. We will call θ the angle defined through $\cos\theta := \frac{k}{K}$. As we are looking for a cusp of size $\frac{1}{K}$, it will be convenient to set $\tilde{U}(y) = U\left(\frac{y}{K}\right)$. It implies that $\frac{1}{K^2}U''\left(\frac{y}{K}\right) = \tilde{U}''(y)$. It comes

$$\left(\frac{d^2}{dy^2} - \cos^2\theta\right)\varphi_\epsilon(y/K, c) + \frac{\beta/K^2 - \tilde{U}''(y)}{\tilde{U}(y) - c - i\epsilon}\varphi_\epsilon(y/K, c) = \frac{\omega(y/K, 0)}{ikK^2(\tilde{U}(y) - c - i\epsilon)}.$$

We set $ikK^2\varphi(y/K, c) := \phi(y, c)$, and the function ω^∞ satisfies

$$\omega^\infty\left(\frac{y}{K}\right) = \omega\left(\frac{y}{K}, 0\right) + \left(\tilde{U}''(y) - \frac{\beta}{K^2}\right)\phi_+(y, c).$$

We see that in the limit of large K , the parameter β completely disappears, it has no effect on the profile. However the solution \tilde{U} still depends on θ . We will first consider the case where the spectrum has only one component θ . Let $w_\theta(y) := \omega^\infty\left(\frac{y}{K}\right)$. The set of equations defining the Reynolds stress divergence $\langle v\omega \rangle [\tilde{U}]$ is

$$\begin{aligned} \left(\frac{d^2}{dy^2} - \tan^2 \theta\right) \phi_\epsilon(y, c) - \frac{\tilde{U}''(y)}{\tilde{U}(y) - c - i\epsilon} \phi_\epsilon(y, c) &= \frac{e^{i \sin \theta y}}{\tilde{U}(y) - c - i\epsilon} \\ e^{i \sin \theta y} + \tilde{U}''(y) \phi_+(y, \tilde{U}(y)) &= w_\theta(y) \\ \frac{1}{\tilde{U}''(y)} [|w_\theta(y)|^2 - 1] &= \langle v\omega \rangle_\theta [\tilde{U}]. \end{aligned} \quad (4.5)$$

The first equation is the inhomogenous Rayleigh equation without β effect. The second one is the modified expression to compute ω^∞ , and the last one is the pseudomomentum balance giving access to the Reynolds stress divergence.

Before we go on with numerical analysis, let us give some analytical results on this set of equations.

- We already gave an expression for the Reynolds stress divergence in the limit $K \rightarrow +\infty$, away from the extremum of the jet. As we have done the scaling $y \leftarrow Ky$, we expect to find the same asymptotic as $y \rightarrow \infty$. For a given profile \tilde{U} , we have the asymptotic result $\langle v\omega \rangle [\tilde{U}] \underset{y \rightarrow \infty}{\sim} -\frac{\tilde{U}''}{\tilde{U}^{\prime 2}}$.

- We know that at the extremum, we have $\omega^\infty(y_{cr}) = 0$ (see subsection 4.1), which corresponds here to $w_\theta(y_{cr}) = 0$. At the extremum, the mean velocity profile is forced by $\langle v\omega \rangle = -\frac{1}{\tilde{U}''}$, it comes from the last equation of (4.5). At a maximum of U (eastward jet), $\tilde{U}'' < 0$ and the Reynolds stress divergence makes the profile \tilde{U} grow. It is the opposite at a minimum of U , we have $\tilde{U}'' > 0$ and the negative velocity grows. The consequence is that the turbulence is always pushing the jet to grow. This growth can be stopped only by either linear friction or non linear effects beyond the quasilinear approximation. For westward jets, we will see further that it can also be stopped by an hydrodynamic instability.

- The formula $\langle v\omega \rangle(y_{cr}) = -\frac{1}{\tilde{U}''(y_{cr})}$ is in itself noteworthy. It comes from the phenomenon of depletion of vorticity at the stationary streamlines, which has been already emphasized in (Bouchet & Morita 2010). To reach the stationary profile, $\langle v\omega \rangle$ has to equilibrate the linear friction. At the extremum of the jet it gives the equality $\langle v\omega \rangle(y_{cr}) = \tilde{U}(y_{cr})$. We can thus link the value of the velocity at the extremum of the jet and the curvature of the cusp. Let us write this equality in its full dimensional form,

$$U(y_{cr}) = -\frac{\epsilon K^2}{r U'''(y_{cr})}, \quad (4.6)$$

where in that formula ϵ is the energy injection rate. This is a universal property of a stationary jet profile, it relates the strength of a jet to its curvature, and the physical parameters ϵ, r and K . It does not depend on θ that characterizes the forcing spectrum through the ratio k/K . Exactly as was the case before when we took the dissipative-small-scale limit, this relation does not depend on the detailed form of the spectrum of the stochastic forcing.

Let us illustrate those results by a numerical computation of the nondimensional equations (4.5). The numerical computation goes the following way: with the solver ode45 of matlab, we write a program solving the first equation of (4.5), for given values of ϵ (the Laplace transform parameter) and c , and given boundary conditions. In our computations, we impose vanishing boundary conditions for ϕ_ϵ and we take a domain

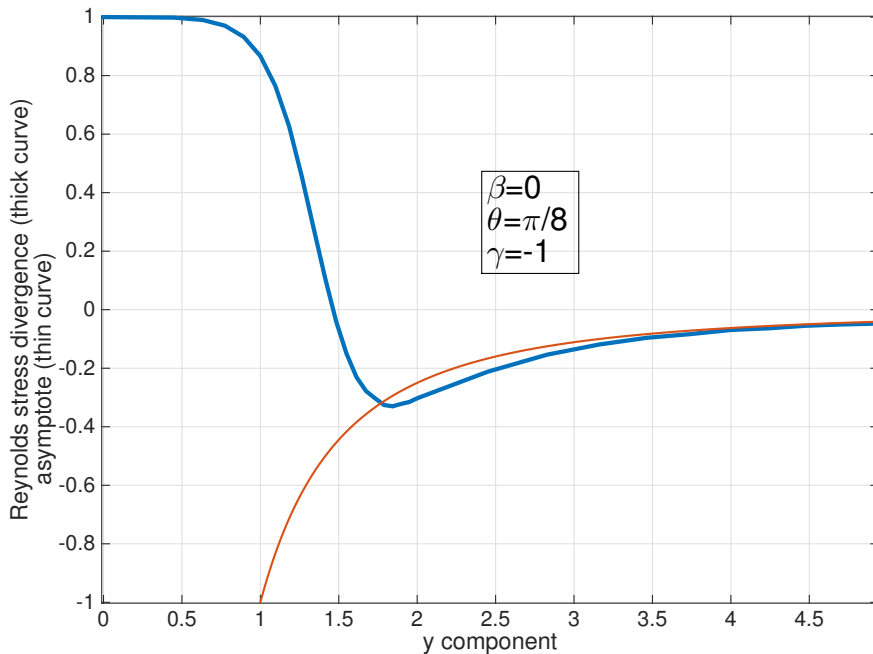


FIGURE 6. Reynolds stress divergence from (4.5) for a parabolic profile $\tilde{U}(y) = -\frac{y^2}{2}$, and $\theta = \frac{\pi}{8}$. (thick curve). The thin curve depicts the theoretical asymptote $\frac{\tilde{U}''}{\tilde{U}^2}$. As one can notice, $\langle v\omega \rangle(0) = -\frac{1}{\tilde{U}''} = 1$ in agreement with the theoretical result.

size $L_y = 30$ which we think to be sufficient to approximate an infinite domain. ϵ has to be small because we want to compute the solution ϕ_+ when ϵ goes to zero. For the results of figure (6), $\epsilon = 10^{-5}$. Because the solution ϕ_+ has a singularity at $U(y_c) = c$, an extreme precision is required to obtain convergence of the numerical calculations. We had to impose 'RelTol'= 10^{-13} and 'AbsTol'= 10^{-15} with the MATLAB solver *odeset*. To obtain the value of $\langle v\omega \rangle_\theta(y)$, we have to compute the solution ϕ_+ for $c = \frac{y^2}{2}$, and this has to be done for each value of y . In figure (6), about 20 values of y were used to plot the blue curve.

The plot of the Reynolds stress divergence in figure (6) clearly displays two regions with a sharp transition at about $y = 2$. For, $y < 2$ the profile should equilibrate to form a cusp, which joins continuously the second region where $y > 2$. In the second region, the expression $\langle v\omega \rangle = -\frac{U''}{U^2}$ seems to be valid, and we expect the profile to join continuously the solution computed in section (3.2) and displayed in figure (4) right. The abscise of the transition to the asymptote $-\frac{U''}{U^2}$ depends on θ , and is thus non-universal with respect to the force spectrum. When θ approaches $\frac{\pi}{2}$, the blue curve reaches the asymptote for larger and larger values of y . This is illustrated in figure (7). The same figure also illustrates the asymetry of $\langle v\omega \rangle_\theta$ w.r.t the transformation $\theta \rightarrow -\theta$. For negative values of θ , the solution oscillates before reaching the asymptotic regime. Note that the set of equations (4.5) is invariant to the transformation $y \rightarrow -y$ and $\theta \rightarrow -\theta$, which means that we do not have to compute the curve for negative values of y , it corresponds to the same curve for positive values of y and the change $\theta \rightarrow -\theta$. In figure (7), we present the curves $\langle v\omega \rangle_\theta$ for different values of θ . Because our algorithm is limited to a domain size $L_y = 30$, we

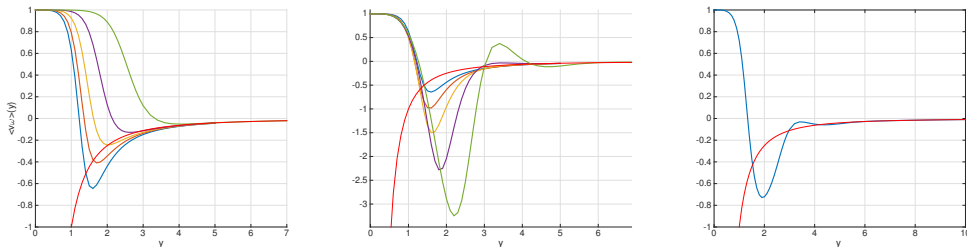


FIGURE 7. Left: The Reynolds stress divergence $\langle v\omega \rangle$ for positive values of θ between 0 and $\pi/3$. From left to right on the picture, the thick curves correspond to values of θ respectively of 0, $\frac{\pi}{12}$, $\frac{2\pi}{12}$, $\frac{3\pi}{12}$, $\frac{4\pi}{12}$. The thin curve displays the asymptote $\frac{U''}{U^2}$. Middle: The Reynolds stress divergence $\langle v\omega \rangle$ for the same but negative values of θ between 0 and $-\pi/3$. Right: The total Reynolds stress divergence resulting from the sum over θ . One can see that the asymptotic behavior is not reached within the range $0 < y < 5$ because of the contribution of the most negative value $\theta = -\pi/3$.

limited our computation to $\theta \in [-\frac{\pi}{3}; \frac{\pi}{3}]$; otherwise the domain of y would be too small for the curve $\langle v\omega \rangle(y)$ to reach its asymptotic regime.

At this point, much remains to do to obtain the real stationary profile of the cusp. We should now use the differential equation

$$\partial_t U = \alpha (\langle v\omega \rangle - U)$$

to compute the stationary profile satisfying $\langle v\omega \rangle[U] = U$. We should use the Reynolds stress divergence $\langle v\omega \rangle$ integrated over θ with the method presented above. The third graph in figure (7) displays the total Reynolds stress divergence after integration over the interval $[-\frac{\pi}{3}, \frac{\pi}{3}]$ with uniform density function (equal weight for all values of θ). We stress that this curve $\langle v\omega \rangle(y)$ is not at all universal, it depends on the spectrum of the stochastic forcing. To compute the total stress tensor with our method, we have to sample the density function of the spectrum, ie to chose enough values of θ and then to sum each contribution. This integration requires much computational effort, maybe even more effort than a direct numerical integration of the S3T equations. Therefore, we think that the set of equations (4.5) is rather a theoretical tool to investigate the general properties of the cusp than a practical way to do an exact computation of the cusp.

With the system of equations (4.5), we have been able to show that a cusp of typical size $\frac{1}{K}$ should exist at the eastward extremum of the jet. This cusp regularizes the velocity profile at its maximum and stops the divergence observed in figure (4). The relation between the curvature of the jet at the extremum and its maximal velocity (4.6) is universal as it does not involve the explicit expression of the spectrum of the stochastic forcing. However, the exact profile of a cusp is rather complicated and is not at all universal. For each particular stochastic forcing, one has to do the whole numerical computation of the Reynolds stress divergence and solve the stationary equation for the velocity profile U .

4.4. Computation of Reynold's stress divergence for westward jets

As we saw in the last section, the parameter β disappears from the equation when we try to compute the equilibrium profile in the limit $K \rightarrow \infty$, because the β effect becomes irrelevant at those scales. Using this approach, we could expect the jet to be symmetric with respect to the transformation $U \rightarrow -U$. At a formal level, nothing in the equations we considered seems to make any difference between the eastward part of a jet

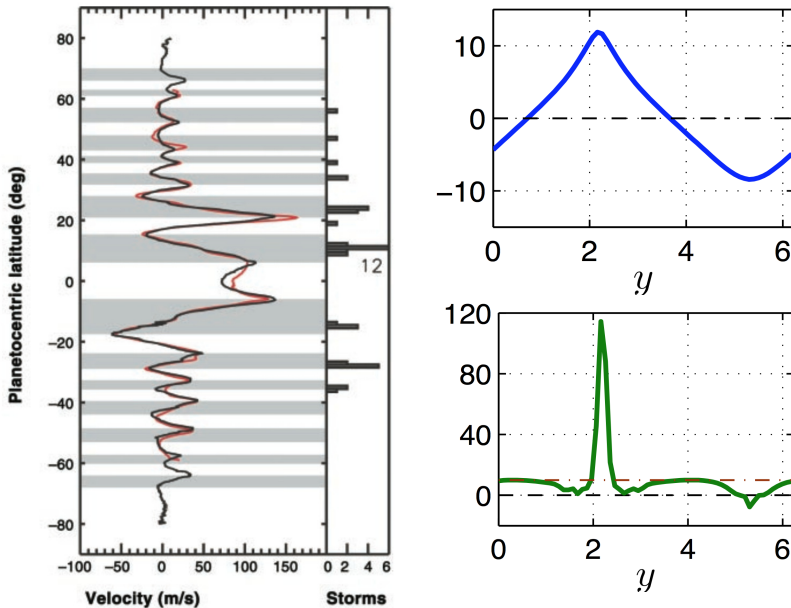


FIGURE 8. Left panel: zonal jets on Jupiter. Data collected by the probes Galileo and Cassini (from (Porco *et al.* 2003)). Right panel: A numerical simulation of the quasilinear barotropic equations (S3T system) performed in (Constantinou 2015). The top figure displays the mean velocity profile U and the bottom figure displays $\beta - U''$. The cusp is obvious on both figures, the peak corresponds to the westward extremum of the jet. $\beta - U''$ is always positive, thus satisfying the Rayleigh-Kuo criterion except possibly at the eastward extremum.

and its westward component. However, if we look at the jets observed on Jupiter, we see a clear asymmetry between eastward and westward jets, especially at high latitudes. One key point will be that, as clearly stated, the computations in (Bouchet & Morita 2010; Bouchet *et al.* 2013) and the previous sections assume that the linearized equations close to the jet are stable, and are modified by the presence of stable neutral modes.

On Jupiter, the cusp only exists on the westward part whereas the eastward part looks like a parabolic profile with curvature between 2β and 3β (see figure (8) and (Ingersoll *et al.* 1981) for a discussion on the value of the curvature). Numerical simulations of the barotropic model also show this asymmetry. Of course, numerical simulations always include a small scale dissipation (usually an hyperviscosity), but as this viscosity is small, we expect the results to be close to those of our model. In (Constantinou 2015) for example, the curvature at the eastward jet is almost exactly β and seems to be trapped at this value whatever large the coefficients K and $\frac{1}{\alpha}$ are. The value of $\beta - U''$ is always positive, and the Rayleigh-Kuo criterion for jet stability is satisfied. The aim of this section is to understand what is the behavior of a parabolic jet with U'' close to β and see if the profile $\beta \frac{y^2}{2}$ can be or not a stationary solution to our equations.

4.4.1. Modified Rossby waves

We consider in equation (4.1) a parabolic profile $U(y) = \gamma \frac{y^2}{2}$, and we want to study the behavior of the Reynolds stress divergence when γ is close to β . For $\gamma = \beta$, any perturbation is carried freely by the mean flow, and equation (2.17) reduces to

$$\partial_t \omega + ikU\omega = 0,$$

which is easily solved by $\omega(y, t) = \omega(y, 0)e^{-ikUt}$. Expression (2.18) is then singular, because $U'' - \beta$ vanishes in the denominator, and $|\omega^\infty|^2 - 1 = |\omega(y, 0)|^2 - 1 = 0$. If we try to compute the Reynolds stress divergence $\langle v\omega \rangle$ directly, we will find a singularity in $y = 0$. Therefore, the aim is to compute $\langle v\omega \rangle$ for γ smaller and larger than β and let then $\gamma \rightarrow \beta$.

It has been proved long ago that for $0 < \gamma < \beta$ we have modified Rossby waves in the flow (Drazin *et al.* 1982), with at least one Rossby wave as soon as $\gamma < \beta$. In (Brunet 1990), the case of a parabolic profile is thoroughly studied and a method is found to compute the Rossby waves and their velocity. Basically, it consists in doing a Fourier transform in y and transform the Rayleigh equation into a one dimensional Schrödinger equation. This one dimensional Schrödinger equation describes a particle in a potential vanishing at infinity. Possible bound states of the Schrödinger equation correspond to modified Rossby waves.

For $\gamma > \beta$, the Schrödinger equation potential is positive, and classical results prove that there is no bound state, and thus there is no Rossby waves. In that case expression (2.18) will be valid to compute the Reynolds stress divergence. By contrast, for $0 < \gamma < \beta$, the Schrödinger equation potential is negative (the position zero is attractive). Classical results (Reed & Simon 1978) shows that there exists a least one bound state, as this is a one-dimensional Schrödinger equation. There is thus at least one modified Rossby wave. Moreover as the potential deepens for decreasing γ/β , the number of bound states and thus the number of modified Rossby waves increases when γ/β decreases. When $0 < \gamma < \beta$, because of the presence of waves, we have to use expression (2.19) to compute the Reynolds stress divergence.

We have used the numerical method described in (Drazin *et al.* 1982), to compute the Rossby waves and we sum up the main results in appendix D.

4.4.2. Singularity of the Reynolds stress

We now compute the stress $\langle v\omega \rangle$ using the same method as for the cusp case discussed in section 4.3, but without taking the limit $K \rightarrow \infty$. It happens that the parabolic profile has an additional symmetry, it is invariant under the transformation $y \leftarrow Ky$. For a parabolic profile, the set of equations only depends on the parameter $\tan\theta := \frac{l}{k}$ and $\mu := 1 - \frac{\beta}{\gamma}$. As discussed previously, Rossby waves appear when $\mu < 0$, or equivalently $0 < \gamma < \beta$.

Now we have to modify expression (2.18) to take into account the presence of those modes and we discuss this problem in more details in appendix A. Using expression (2.19), the self-consistent equations for the jet write

$$\begin{aligned} \left(\frac{d^2}{dy^2} - \tan^2 \theta \right) \phi_\epsilon(y, c) - \frac{\mu}{\frac{y^2}{2} - c - i\epsilon} \phi_\epsilon(y, c) &= \frac{\mathcal{P}e^{i \sin \theta y}}{\frac{y^2}{2} - c - i\epsilon} \\ \mathcal{P}e^{i \sin \theta y} + \mu \phi_+ \left(y, \frac{y^2}{2} \right) &= w_\theta(y) \\ \frac{1}{\mu} \left[(1 - \mathcal{P}) e^{i \sin \theta y} \right]^2 + |w_\theta(y)|^2 - 1 &= \frac{1}{\gamma} \langle v\omega \rangle_\theta [\tilde{U}]. \end{aligned} \quad (4.7)$$

We have denoted by \mathcal{P} the projector on the space orthogonal to the neutral modes. The reader should notice that the quantity $\frac{1}{\gamma} \langle v\omega \rangle_\theta$ depends on β and γ only through the parameter μ . The computation of the Reynolds stress divergence for a parabolic profile in the β plane resumes to the normal profile $\frac{y^2}{2}$ and an other control parameter μ .

The result of the numerical integration of (4.7) is shown in figure (9). The main result is that the stress $\langle v\omega \rangle$ has the same qualitative behavior both for $\gamma < \beta$ and for $\gamma > \beta$.

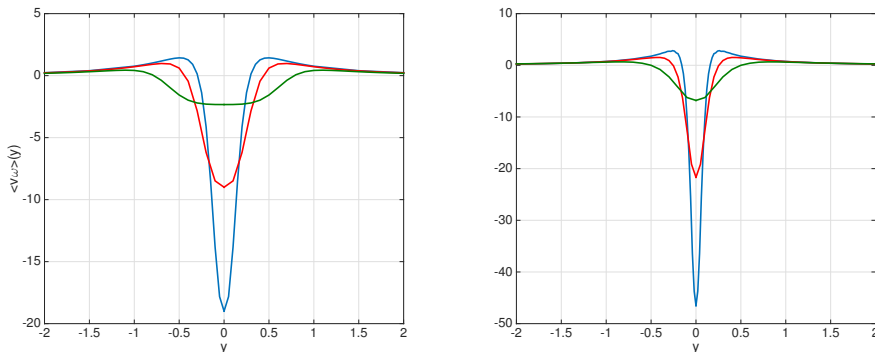


FIGURE 9. Left: Minus the Reynolds stress divergence $\langle v\omega \rangle$ obtained for $\mu = 0.3$ (green), $\mu = 0.1$ (red) and $\mu = 0.05$ (blue). When the parameter μ comes closer to zero, the divergence at $y = 0$ becomes more and more pronounced. Right: The Reynolds stress divergence for $\mu = -0.3$ (green), $\mu = -0.1$ (red) and $\mu = -0.05$ (blue). Other parameters are $\theta = \frac{\pi}{8}$ and $\beta = 1$.

For $\gamma > \beta$, i.e $\mu > 0$, we still have the result that $w_\theta(0) = 0$, which implies that the stress $\langle v\omega \rangle$ is diverging as $-\frac{1}{\mu}$ when $\mu \rightarrow 0^+$. For $0 < \gamma < \beta$, i.e $\mu < 0$, the stress is diverging as $\frac{[\omega_\theta^1(0)]^2 - 1}{\mu}$ when $\mu \rightarrow 0^-$. ω_θ^1 is the projection of $e^{i \sin y}$ on the first neutral mode. It happens that $|\omega_\theta^1(0)|^2 - 1$ is always positive. Hence, $\frac{[\omega_\theta^1(0)]^2 - 1}{\mu}$ is negative. We conclude that whatever the sign of μ , the stress $\langle v\omega \rangle$ has a negative divergence at the minimum of the jet that makes the jet grow. If the curvature γ is smaller than β , the effect of the Reynolds stress divergence is to narrow the jet and increase the curvature. It will come to a point where $\gamma > \beta$ and the Rayleigh-Kuo criterion of stability will be violated. No mechanism in our present model can stop the growth of the westward jet. The jet should create a cusp exactly the same way as for the eastward jet. To explain the numerical simulations, we thus have to consider other hypothesis than the ones we did. Among those, we have assumed there is no instability in the set of equations (4.7), i.e a mode with nonzero imaginary part of the velocity. When the Rayleigh-Kuo criterion is violated, the stability of a jet is no longer guaranteed, and instabilities may occur. In the last section of this paper, we will study qualitatively the effect of an instability to see whether it can really stop the growth of the westward jet.

4.4.3. The question of the instability in the westward jet

We discussed previously (in appendix A) how the Reynolds stress divergence is modified when there are modified Rossby waves in the flow. Rossby waves are regular solutions of the homogeneous Rayleigh equation

$$\left(\frac{\partial^2}{\partial y^2} - k^2 \right) \psi + \frac{\beta - U''}{U - c} \psi = 0, \quad (4.8)$$

where c is the phase speed of those modes. Modified Rossby waves are called *neutral* modes because the phase speed is real. An unstable mode would be a solution of equation (4.8) with *complex* phase speed c . In particular for unstable modes, the imaginary part satisfies $kc_i > 0$ and the consequence of that is the exponential growth of a disturbance $|\psi(y, t)| \propto e^{kc_i t}$. The Rayleigh-Kuo criterion has to be violated in the flow, this is a well known necessary condition for instability (see e.g (Pedlosky 1982)). This condition is not sufficient but if we assume an unstable mode exists, expression (2.19) will not be valid anymore, because the unstable mode has a contribution in the stress. This contribution is

not at all trivial. If we take the limit $\alpha \rightarrow 0$ in the presence of such a mode, the Reynolds stress is diverging because there is no mechanism to compensate the exponential growth of the unstable mode. To obtain a finite value of the Reynolds stress, we assume that the flow equilibrates in a state for which $kc_i < \alpha$. This would correspond to a situation of marginal instability, a kind of barotropic adjustment mechanism. The computation is similar to the one developed in appendix A for neutral modes. There will be a term coming from the unstable mode alone, and cross terms coming from the contribution mode-continuum. Contrary to what happens for Rossby waves, we cannot assume that the cross contributions vanishes because for an unstable mode, the real part c_r of the speed c lies within the range of U ((Drazin & Reid 2004; Drazin *et al.* 1982)). However, the computation shows that the cross term mode-continuum is small compared to the contribution mode-mode except perhaps in a region where $k(U(y) - c_r)$ is of order α . The contribution of an instability in the Reynolds stress has been already computed in the deterministic case ((Pedlosky 1982) p 576), and we modify here the classical result to adapt it to the stochastic case.

Let $\omega^c(y)$ be the projection of the initial condition e^{ily} on the unstable mode, and ψ^c the associated stream function defined by $\left(\frac{\partial^2}{\partial y^2} - k^2\right)\psi^c = \omega^c$. The projection refers to the scalar product induced by the pseudomomentum conservation law (see appendix A for the discussion). Then the term mode-mode in the computation of $2\alpha \langle |\omega|^2 \rangle$ writes

$$\begin{aligned} 2\alpha \langle |\omega|^2 \rangle &= 2\alpha \int_{-\infty}^0 dt e^{2\alpha t} |\omega^c(y) e^{ikct}|^2 \\ &= |\omega^c(y)|^2 \frac{2\alpha}{2\alpha - 2kc_i}. \end{aligned}$$

Equation (4.8) shows that $\omega^c = -\frac{\beta - U''}{U - c} \psi^c$. Therefore, we have a contribution to the Reynolds stress divergence

$$\frac{2\alpha \langle |\omega|^2 \rangle}{U'' - \beta} = -\frac{2\alpha}{2\alpha - 2kc_i} \frac{|\psi^c|^2}{|U - c|^2} (\beta - U''). \quad (4.9)$$

Let us emphasize once more that this term is a *contribution* to the Reynolds stress adding to the other terms coming from the effect of Rossby waves and from $\tilde{\omega}^\infty$. The important point in (4.9) is that the coefficient $\frac{2\alpha}{2\alpha - 2kc_i} \frac{|\psi^c|^2}{|U - c|^2}$ is strictly positive, which means that the term coming from the unstable mode *opposes* a change of sign of $\beta - U''$. In the numerical simulations, we see that the profile U tends to satisfy the Rayleigh-Kuo criterion with $\beta - U'' > 0$ in the flow except perhaps at the extremum of the westward jet. Then in section 4.4.2 we have shown that a parabolic profile U with curvature $\gamma < \beta$ but close to β is forced by a Reynolds stress divergence with a kind of singularity at zero (see figure (9), right). The effect of the stress is to increase the jet and makes it violate the Rayleigh-Kuo criterion. In order to equilibrate, the jet needs another mechanism to compensate this forcing. Our analysis thus allows us to make the qualitative following statements:

If the Rayleigh-Kuo criterion is violated at the westward jet and if an hydrodynamic instability develops, then the instability tends to reequilibrate the flow to a configuration for which the flow is stable, with $\beta - U'' > 0$.

Please note that this probably makes our assumption of marginal stability kc_i of order α self-consistent.

In order to illustrate this assertion and go a bit further in the above description of the instability mechanism, we tried to find numerically a configuration where the instability

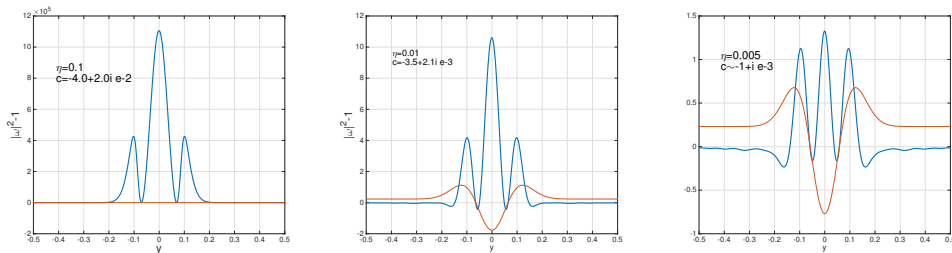


FIGURE 10. We show here the tensor $|\omega|^2 - 1$ at $T = 30$ for different values of η , and we compute the value of c if possible. The thinner curve (red color online) shows $\beta - U''$. Close to the instability threshold, it is no longer possible to determine the value of c because the growth of the instability is too slow.

develops. We perform a direct numerical integration of the equation

$$\partial_t \omega + ikU\omega + ik(\beta - U'')\psi = 0,$$

using periodic boundary conditions in y for the solution $\omega(y, t)$ and the initial condition $\omega(y, 0) = e^{ily}$. We use a Runge-Kutta algorithm of order 4. The profile U is parabolic with $0 < \gamma < \beta$ but we add a small disturbance at the extremum in 0 of the form of a gaussian $-\eta e^{-\frac{y^2}{\sigma^2}}$. This disturbance is the qualitative effect of the forcing described in figure (9), it models the fact that the mean velocity profile is “curved” at its extremum.

$$U(y) = \gamma \frac{y^2}{2} - \eta e^{-\frac{y^2}{\sigma^2}}. \quad (4.10)$$

The values of the chosen parameters are $\beta = 1$, $\mu = 1 - \frac{\beta}{\gamma} = -0.3$, $k = l = 10$, and the box size is $L_y = 10$. σ quantifies the width of the disturbance, we chose $\sigma = 0.1$. The solution $\omega(y, t)$ is oscillating very fast in y at long times because of the contribution of e^{-ikUt} , and it imposes a very high spatial resolution. With $N_y = 2.10^4$ we obtain satisfactory results as long as $t < 100$. We have a time step $dt = 10^{-3}$. η describes the magnitude of the disturbance, this is the parameter we will vary. Results are displayed in figure (10). The red curve is the graph of $\beta - U''(y)$. When this quantity is strictly positive everywhere in the flow, the Rayleigh-Kuo criterion is satisfied and the flow is stable. With the velocity profile chosen in (4.10), the Rayleigh-Kuo criterion is violated around $y = 0$ because the red curve crosses the ordinate zero. The blue curve displays the quantity $|\omega|^2(y, t) - 1$ at $T = 30$. In our simulations, we clearly see the three peaks of the blue curve growing exponentially with time, and this indicates the existence of an hydrodynamic instability. From left to right, we have increased the value of the parameter η . The larger η , the more the Rayleigh-Kuo criterion is violated, and the instability grows faster. It has been already emphasized that $|\omega|^2 - 1$ has to vanish at the same time where $\beta - U'' = 0$ in the flow, and this is confirmed by our simulation and displayed in figure (10). The largest peak of the blue curve corresponds exactly to the region in the flow where $\beta - U''$ is negative.

As soon as $\eta > 0.003$ we can see the instability growing in the reynolds stress divergence. The value corresponds to a violation of the Rayleigh-Kuo criterion in the vicinity of $y = 0$. When we increase the values of η , the magnitude c_i of the instability increases as well, as we expected. At long time, the dominant contribution in ω is given by the unstable mode $\omega(y, t) \sim \omega^c(y)e^{-ikct}$. Hence the value of $\frac{\dot{\omega}}{\omega}$ gives access to the coefficient ikc . To obtain the mode $\omega^c(y)$, we simply look at the convergence of $\omega(y, t)e^{ikct}$. The real and imaginary parts of the unstable mode $\omega^c(y)$ are displayed

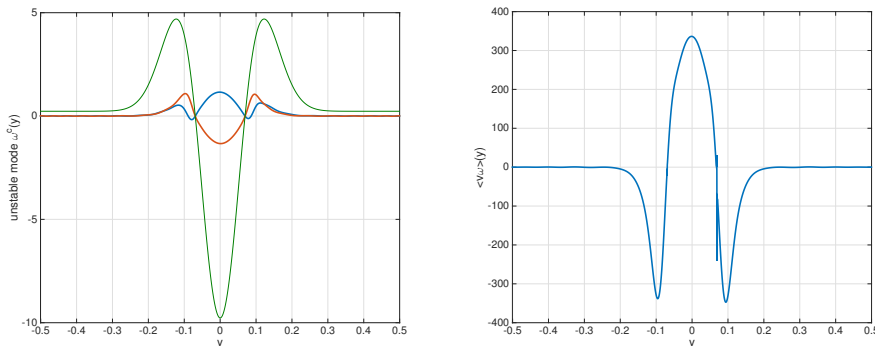


FIGURE 11. Left: real part (blue curve) and imaginary part (red curve) of the unstable mode ω^c . The value of η is 0.05. The thinner curve (green) displays $\beta - U''(y)$, the Rayleigh-Kuo criterion is violated in the vicinity of zero. Right: The tensor $\frac{|\omega|^2 - 1}{U'' - \beta}$ that contributes to the Reynolds stress divergence obtained for $T=30$. The artefact comes from the fact that $U'' - \beta$ vanishes and that we use a finite discretisation in y . The effect of this tensor is to reequilibrate the velocity U to satisfy $\beta - U'' > 0$. The value of c is $c = -2.02 + 1.04i e - 2$

in figure (11) left panel in respectively blue and red. The curve $\beta - U''$ has been superimposed in yellow. We see again that the unstable mode is vanishing at points where $\beta - U'' = 0$ and that the mode is larger in the region where $\beta - U'' < 0$. On the right panel of figure (11) we display the Reynolds stress divergence $\langle v\omega \rangle = \frac{|\omega|^2 - 1}{U'' - \beta}$ obtained from equation (2.18) with one single Fourier component. As can be checked directly in figure (11) right, the effect of the instability is exactly the opposite as on figure (9). The Reynolds stress divergence is positive in the region where the Rayleigh-Kuo criterion is violated, and thus the tensor in figure (11) reequilibrates the profile U and damps the perturbation $-\eta e^{-\frac{y^2}{\sigma^2}}$.

Let us summarize the results of the last section. We have first investigated the behavior of the Reynolds stress divergence for a parabolic profile, because we know from numerical simulations that the mean velocity profile is close from parabolic for a westward jet. The Reynolds stress divergence is the tensor that forces the mean flow according to equation (2.2). Even if we cannot always compute exactly this tensor, we can study its sign and its qualitative properties to see if it damps the flow or if it makes it grow. We did first the assumption that there is no hydrodynamic instability in the flow, that means that there is no unstable mode growing exponentially. But this assumption leads to a contradiction for the parabolic profile because the Reynolds stress divergence distorts the parabolic profile at $y = 0$ as was shown in figure (9). Thus, we conclude that another mechanism is at place to equilibrate the parabolic profile. When we consider a small violation of the Rayleigh-Kuo criterion near $y = 0$, we see numerically the growth of an instability that opposes exactly to the distortion of the parabolic profile where the Rayleigh-Kuo criterion is violated. Those results are qualitative, we do not have computed the velocity profile at equilibrium. But it is consistent to assume that the equilibration mechanism is a kind of barotropic adjustment of the mean flow: an instability develops as soon as $\beta - U''$ changes sign. The flow has to adjust itself such that the instability is not too large, i.e close to a parabolic profile with $U'' \sim \beta$, and such that the instability can be damped by the linear friction.

5. Conclusion and perspectives

The quasilinear barotropic equations in a β plane can lead to formation and equilibration of zonal jets. Those jets are in an out of equilibrium steady state that results in a balance between energy injection at small scales and linear friction that dissipates energy at large scales. With the quasilinear approximation, there is no inverse energy cascade in Fourier space and energy is directly transferred from small scales to the mean flow. After rescaling of the equations, two nondimensional parameters remain, α and K , where α gives the ratio of the time scale for energy injection and dissipation over the inertial time scale and $\frac{1}{K}$ gives the scale of the stochastic forcing. From astronomical observations on Jupiter, we believe that both limits $\alpha \rightarrow 0$ and $K \rightarrow \infty$ are relevant to describe planetary flows.

The presence of the small parameters $\alpha, \frac{1}{K}$ in the equations allows us to perform asymptotic calculations and derive explicit expressions for the Reynolds stress tensor $\langle uv \rangle$. More precisely, we show that for a monotonic mean velocity profile U , both limits commute and give the same expression for the Reynolds stress $\langle uv \rangle = \frac{\epsilon}{U'}$, where ϵ is the energy injection rate in $m^2 s^{-3}$ and U' is the spatial derivative of U . We explained in this paper the physical meaning of this relation: $U' \langle uv \rangle$ is the energy rate transferred to the mean flow by the eddies. With vanishing dissipation and small scale forcing, *all* energy has to be transferred *locally* in space to the mean flow. Thus we obtained for the Reynolds stress a kind of universal relation because it does not depend any more on the detailed spectrum of the forcing.

Because jets are nonmonotonic velocity profiles, the asymptotic expansion breaks down at the extrema. The first naive computation of the velocity profile in the limit $K \rightarrow \infty$ leads to a divergence of the velocity at the extremum. For the asymptotic expansion to be valid, the parameter $\frac{U''}{K\alpha}$ has to remain small. But at the extremum, the velocity profile is regularized by a small scale structure, a cusp, where U'' scales typically like K^2 and therefore the parameter $\frac{U''}{K\alpha}$ is always large at the extremum of eastward jets where the cusp develops. We studied therefore the inertial limit $\alpha \rightarrow 0$ and we derived a system of equations that describes the velocity profile of the cusp. No universal behavior is expected for a cusp, the shape should depend on the precise spectrum of the stochastic forcing. Nevertheless, the mechanism of depletion of vorticity at the stationary streamlines leads to an interesting relation between the curvature of a cusp and the maximal velocity $U(y_{cr}) = -\frac{\epsilon K^2}{r U''(y_{cr})}$. This relation is 'universal' because only the energy injection rate and the scale of the forcing appear explicitly.

Surprisingly, no numerical simulations display a cusp for westward jets whereas our equations for the cusp predict that if U is solution, $-U$ should also be a solution. The physical mechanism that prevents westward jets from creating a cusp is an hydrodynamic instability. When a cusp starts to develop, the Rayleigh-Kuo criterion of stability is violated at the extremum and an hydrodynamic instability grows. Supported by numerical simulations, our claim is that the parabolic profile observed for westward jets is the result of a marginal stability: without instability, the Reynolds stress divergence enhances the mean flow. But as soon as the mean flow has a curvature $U'' > \beta$, the hydrodynamic instability opposes the growth of the velocity profile. Therefore, the parabolic profile is stabilized with a curvature around β resulting of the competition of the two previous mechanisms.

Westward jets on Jupiter display indeed a parabolic profile, but with a curvature U'' clearly larger than β . This is one reason why the barotropic model is not sufficient to describe Jupiter's atmosphere. We believe our analysis could be extended to more refined models, for example a two-layer model. If the aim is to obtain quantitative results about

the velocity profile of Jupiter, one would have to go further in numerical computations than we did. It would be interesting to find numerically the equilibrium profile of a cusp, and then check that this profile is indeed solution of the set of equations (4.7).

In this paper, we have considered the case of a Rayleigh friction as the mechanism for removing energy that is transferred to the largest scale. Rayleigh friction is a rather ad-hoc type of damping (although it can be justified in certain cases involving, e.g., Ekman pumping). If one would consider other kinds of friction, for instance scale-selective damping, provided that this damping actually acts on the largest scales of the flow, in a corresponding inertial limit we expect most of our results to easily generalize (the proper dissipation operator should then replace Rayleigh friction in equation (2.1)). Indeed the processes that explain the computation of the Reynolds stress are inertial in nature and independent from the dissipation mechanisms. As an example, the case of viscous dissipation has been discussed in section 5.1.2 of Bouchet *et al.* (2013), showing that while the regularization by viscosity is very different from the regularization by linear friction, the inertial results for the Reynolds stresses do coincide. This is true as far as the shear is non zero and equation (1.1) is concerned; by contrast the regularization of the cusp is dissipation dependent. In some specific cases, changing the dissipation mechanism may induce specific instability modes, like boundary layer modes due to viscous dissipation, however such effects are expected to be non generic.

This work was thought to be the first step toward a general comprehension of the statistical properties of zonal jets. What we have done here is to compute the averaged Reynolds stress $\langle uv \rangle$ wrt the realizations of the stochastic force. However, it is known from numerical simulations that the mean flow U can have more than one stable stationary state, with a different number of jets. With a stochastic forcing, the system can do transitions between those different states, with however a small probability. To understand the rare transitions between states with a different number of jets, one would have to go beyond the averaging procedure and study also the fluctuations and large deviations of the Reynolds stress. On Jupiter, there are some clues that one jet has been lost in the past, which indicates that transitions similar to those observed in our numerical simulations could really happen in real systems. Numerical work is in progress to study the appearance or disappearance of a jet, and much remains to be done in theory.

We thank P. Ioannou for interesting discussion during the preliminary stage of this work.

The research leading to these results has received funding from the European Research Council under the European Union's seventh Framework Program (FP7/2007-2013 Grant Agreement No. 616811).

Appendix A. The Reynolds stress divergence in the inertial limit

The aim of this section is to give the proof of formula (2.18) and (2.19). We have to compute

$$2\alpha \langle |\omega|^2 \rangle = 2\alpha \int_{-\infty}^0 dt e^{2\alpha t} |e^{tL_k}[c_l]|^2, \quad (\text{A } 1)$$

where $e^{tL_k}[c_l] := \omega_d$ is the solution to the deterministic equation

$$\begin{aligned} \partial_t \omega_d + ikU\omega_d + ik(\beta - U'')\psi_d &= 0 \\ (\partial_y^2 - k^2)\psi_d &= \omega_d \end{aligned} \quad (\text{A } 2)$$

with initial condition $c_l(y) = e^{ily}$. We will first assume there are no neutral modes solutions of (A 2). First, we do the change of time scale $2\alpha t \rightarrow t$ in the integral of (A 1). It gives us

$$2\alpha \langle |\omega|^2 \rangle = \int_{-\infty}^0 dt e^t \left| e^{\frac{t}{2\alpha} L_k} [c_l] \right|^2.$$

When α goes to zero, the term $e^{\frac{t}{2\alpha} L_k} [c_l]$ is the long time limit of the solution of (A 2). We use the nontrivial result for the case of non monotonous flows, of (Bouchet & Morita 2010) already mentioned, that there exists a function $\omega_d^\infty(y)$ such that $\omega_d(y, t) \underset{t \rightarrow \infty}{\sim} \omega_d^\infty(y) e^{-ikU t}$ when there are no neutral modes. Hence $\left| e^{\frac{t}{2\alpha} L_k} [c_l] \right| \rightarrow |\omega_d^\infty(y)|$, and the presence of the exponential in the integral ensures the convergence of the whole. This proves that without neutral modes

$$2\alpha \langle |\omega|^2 \rangle \xrightarrow{\alpha \rightarrow 0} |\omega_d^\infty|^2.$$

The second case, with neutral modes, is a bit more subtle. The result of (Bouchet & Morita 2010) relies on a Laplace transform of ω_d denoted $\hat{\omega}_d$. To do the inverse Laplace transform, one has to know where the singularities of $\hat{\omega}_d$ are. The presence of modes in the equation is exactly equivalent to the presence of poles of order 1 in the complex plane for $\hat{\omega}_d$. For unstable modes, these poles have an imaginary part, whereas for neutral modes, they are located on the real axis. We also assume in our calculation that there are no instabilities, which means that all singularities of $\hat{\omega}_d$ are on the real axis. Some of these singularities are outside the range of U (outside of $[U_{min}, U_{max}]$) and are isolated, they correspond to neutral modes or “modified Rossby waves”. But there is also a continuum of singularities all along the range of U . The integration around the isolated singularities will give the contribution of neutral modes, and it is of the form $\sum_a \omega^a(y) e^{ikc_a t}$ where a is the mode index, c_a is the mode frequency, and the $\omega^a(y)$ are the projections of the initial condition e_l on the modes $\zeta^a(y)$. The projections are defined with the natural scalar product induced by the pseudomomentum conservation law, that is $\ll \omega_1^* \omega_2 \gg = \int \frac{\omega_1^* \omega_2}{U'' - \beta} dy$. For this particular scalar product, the operator $\omega \rightarrow U\omega + (\beta - U'')\psi$ is self-adjoint, and this implies that its eigenvectors are orthogonal with respect to this scalar product. If we subtract the contribution of the modes from c_l , we leave only the continuum part of the singularities and the result of Bouchet and Morita (Bouchet & Morita 2010) holds. There should exist a function $\tilde{\omega}_d^\infty(y)$ such that the remaining part of the solution behaves at infinity like $\tilde{\omega}_d^\infty(y) e^{-ikU(y)t}$. We eventually find that for long time, the solution of the deterministic equation behaves like

$$\omega_d(y, t) \underset{t \rightarrow \infty}{\sim} \sum_a \omega^a(y) e^{-ikc_a t} + \tilde{\omega}_d^\infty(y) e^{-ikU(y)t}.$$

When we inject this result in the expression of $\left| e^{\frac{t}{\alpha} L_k} [e_l] \right|^2$ we get three different terms.

(i) Terms coming from the mode-mode contribution of the form $\sum_a |\omega^a(y)|^2$. The time integration is then trivial.

(ii) Also the term coming from the continuum gives us immediately the contribution $|\tilde{\omega}_d^\infty(y)|^2$.

(iii) What happens for terms of the form $\omega^{a*} \tilde{\omega}^\infty e^{-ik(U-c_a)\frac{t}{\alpha}}$ and $\omega^{a*} \omega^b e^{-ik(c_b-c_a)\frac{t}{\alpha}}$? The frequencies $\frac{1}{\alpha} k(U - c_a)$ and $\frac{1}{\alpha} k(c_a - c_b)$ grow to infinity as α vanishes. We have an oscillating integral with frequency growing to infinity, so its a well known result that such an integral is vanishing. The cross terms give no contributions.

We have then proved the desired result that

$$2\alpha \langle |\omega|^2 \rangle \xrightarrow{\alpha \rightarrow 0} \sum_a |\omega^a|^2 + |\tilde{\omega}_d^\infty|^2.$$

Appendix B. Computation of the Reynolds stress in the small scale forcing regime

The aim of this section is to compute an asymptotic expression for the Reynolds stress when $K \rightarrow \infty$. We will give a proof of equation (3.1).

Let us first recall the two expressions, defined in section 3, that we will use in the computation

$$\partial_t A_{k,l} = -i \frac{U'' - \beta}{k} \int dY H_0(Y) A_{k,l} \left(y - \frac{Y}{k}, t \right) e^{ik(U(y) - U(y - \frac{Y}{k}))t}, \quad (\text{B } 1)$$

with initial condition $A_{k,l}(y, 0) = e^{ily}$ and the quantity $2\alpha \langle |\omega|_{k,l}^2 \rangle$ that appears in the Reynolds stress divergence (2.13)

$$2\alpha \langle |\omega_{k,l}|^2 \rangle = 2\alpha \int_0^{+\infty} e^{-2\alpha t} |A_{k,l}(y, t)|^2 dt.$$

Again, the bracket $\langle \rangle$ is simply a stochastic averaging. An integration by parts gives

$$2\alpha \langle |\omega_{k,l}|^2 \rangle = |A_{k,l}(y, 0)|^2 + 2\mathcal{Re} \int_0^{+\infty} e^{-2\alpha t} A_{k,l}(y, t)^* \partial_t A_{k,l}(y, t) dt.$$

Because $|A_{k,l}(y, 0)|^2 = 1$, it compensates exactly the -1 coming from the enstrophy injection in expression (2.13). Replacing $\partial_t A_{k,l}$ using (B 1) and equation (2.13) that gives the expression of $\mathcal{Re} \langle v_{k,l} \omega_{k,l}^* \rangle$, we get the *exact* expression for the Reynolds stress divergence

$$\mathcal{Re} \langle v_{k,l} \omega_{k,l}^* \rangle = \frac{\hat{C}_{k,l}}{k} \mathcal{Im} \int_0^{+\infty} dt \int dY H_0(Y) A_{k,l}^*(y, t) A_{k,l} \left(y - \frac{Y}{k}, t \right) e^{ik(U(y) - U(y - \frac{Y}{k}))t} e^{-2\alpha t}.$$

Now we will have to use our hypothesis $K \rightarrow \infty$ to go on in the computation. Here comes a small subtlety, the l component does not appears explicitly, it is hidden in the initial condition $A_{k,l}(y, 0) = e^{ily}$. Therefore we cannot just expand $A_{k,l}(y - \frac{Y}{k}, t)$ in power of $\frac{1}{k}$ as one may guess at first sight. But expression (B 1) tells us that $\partial_t A_{k,l} \rightarrow 0$ as K goes to infinity. The right way to do the asymptotic expansion consists in an expansion of $A_{k,l}(y, t)$ wrt time and we use that each temporal derivation of $A_{k,l}$ is smaller of order $\frac{1}{K}$

$$\begin{aligned} A_{k,l}^*(y, t) A_{k,l} \left(y - \frac{Y}{k}, t \right) &= A_{k,l}^*(y, 0) A_{k,l} \left(y - \frac{Y}{k}, 0 \right) \\ &\quad + t \partial_t \left[A_{k,l}^*(y, t) A_{k,l} \left(y - \frac{Y}{k}, t \right) \right]_{t=0} + O\left(\frac{1}{K^2}\right), \end{aligned}$$

and we expand also U using that k is large

$$\begin{aligned} k \left(U(y) - U\left(y - \frac{Y}{k}\right) \right) &= U'(y)Y - \frac{U''(y)}{2k} Y^2 \\ &:= aY - bY^2. \end{aligned}$$

The last expression defines a and b . Using that $A_{k,l}(y, 0) = e^{ily}$, $H_0(Y) = \frac{1}{2}e^{-|Y|}$ for infinite space, the first nonzero contribution is given by

$$\mathcal{R}e \langle v_{k,l} \omega_{k,l}^* \rangle \underset{K \uparrow \infty}{\sim} \frac{\hat{C}_{k,l}}{2k} \mathcal{I}m \int_0^{+\infty} dt \int dY e^{-|Y|} e^{-iY \tan \theta} e^{i(aY - bY^2)t} e^{-2\alpha t}, \quad (\text{B } 2)$$

with $\tan \theta = \frac{l}{k}$. One could check easily that the expression (B 2) is zero when $b = 0$, that's why we have to keep the b term to get the leading order term in the expansion in powers of $1/K$.

We now prove that the second term in the expansion of $A_{k,l}^*(y, t)A_{k,l}(y - \frac{Y}{k}, t)$ is zero. With expression (B 1), we compute

$$\partial_t A_{k,l}(y, 0) = -i \frac{U'' - \beta}{k} \frac{e^{ily}}{1 + \tan^2 \theta},$$

and then

$$\begin{aligned} A_{k,l}^*(y, 0) \partial_t A_{k,l} \left(y - \frac{Y}{k}, 0 \right) &= -i \frac{U'' - \beta}{k} \frac{e^{-il \frac{Y}{k}}}{1 + \tan^2 \theta} \\ \partial_t A_{k,l}^*(y, 0) A_{k,l} \left(y - \frac{Y}{k}, 0 \right) &= i \frac{U'' - \beta}{k} \frac{e^{-il \frac{Y}{k}}}{1 + \tan^2 \theta} \end{aligned}$$

The sum of both terms is zero. The next contribution then implies two derivatives and is of order $\frac{1}{K^2}$.

The presence of both exponentials in (B 2) allows us to invert the order of integration and integrate the time first. We get

$$\mathcal{R}e \langle v_{k,l} \omega_{k,l}^* \rangle \underset{K \uparrow \infty}{\sim} \frac{\hat{C}_{k,l}}{2k} \mathcal{I}m \int dY \frac{e^{-|Y|} e^{-iY \tan \theta}}{2\alpha - i(aY - bY^2)}.$$

Now we have to use that $b := \frac{U''}{2k}$ is small and develop the denominator. This gives

$$\begin{aligned} \mathcal{R}e \langle v_{k,l} \omega_{k,l}^* \rangle \underset{K \uparrow \infty}{\sim} \frac{\hat{C}_{k,l}}{2k} \mathcal{I}m \int dY \frac{e^{-|Y|} e^{-iY \tan \theta}}{2\alpha - iaY + ibY^2} \\ \underset{K \uparrow \infty}{\sim} -\frac{\hat{C}_{k,l}}{2k} \mathcal{I}m \int dY bY^2 \frac{\partial}{\partial(aY)} \left\{ \frac{e^{-|Y|} e^{-iY \tan \theta}}{2\alpha - iaY} \right\}. \end{aligned}$$

Now comes a trick: $U''Y^2 \frac{\partial}{\partial(U'Y)} = Y \frac{\partial(U'(y)Y)}{\partial y} \frac{\partial}{\partial(U'(y)Y)} = Y \frac{\partial}{\partial y}$ and, recalling that $b = U''/2k$, we can put the derivative in y in front of the integral. This is a method to recognize that our expression is a derivative in y and get the analytic expression of the Reynolds stress. The idea to recognize a derivative seems to fall from nowhere, but it comes in fact from the work (Srinivasan & Young 2014) and the expression they derived for the Reynolds stress. In Fourier space, the incompressibility condition writes $\mathcal{R}e \langle v_{k,l} \omega_{k,l}^* \rangle = -\partial_y \mathcal{R}e \langle u_{k,l} v_{k,l}^* \rangle$, we then get

$$-\partial_y \mathcal{R}e \langle u_{k,l} v_{k,l}^* \rangle \underset{K \uparrow \infty}{\sim} -\frac{\hat{C}_{k,l}}{4k^2} \frac{\partial}{\partial y} \mathcal{I}m \int dY \frac{Y e^{-|Y|} e^{-iY \tan \theta}}{2\alpha - iaY}$$

and finally

$$\mathcal{R}e \langle u_{k,l} v_{k,l}^* \rangle \underset{K \uparrow \infty}{\sim} C + \frac{\hat{C}_{k,l}}{4k^2} \mathcal{I}m \int dY \frac{Y e^{-|Y|} e^{-iY \tan \theta}}{2\alpha - iaY}.$$

The integration procedure defines $\langle uv \rangle$ up to a constant. This constant has no influence on the solution of equation (2.2). We are considering an unbounded space in the y -direction.

Consider a profile U such that $U \rightarrow U_0$ at infinity. The Reynolds stress is vanishing for a constant velocity profile, and this implies that the integration constant is zero. In general, the expression of the Reynolds stress will depend on the boundary conditions.

Appendix C. Equivalence of the inertial small-scale regime and the dissipative small-scale regime for monotonic profiles

In this appendix we prove that

$$\mathcal{R}e \langle v_\theta^* \omega_\theta \rangle \xrightarrow{K \rightarrow \infty, \alpha \rightarrow 0} \frac{U''}{U'^2}.$$

In section 4, we found the expression

$$\mathcal{R}e \langle v_\theta^* \omega_\theta \rangle \underset{K \rightarrow \infty}{\sim} -\frac{\hat{C}_{k,l}}{2k^2} \mathcal{P} \left\{ \int dY e^{-|Y|} \frac{\cos(Y \tan \theta)}{U(y - \frac{Y}{k}) - U(y)} \right\}.$$

This expression has no meaning for y_c such that $U'(y_c) = 0$ because we have a quadratic singularity in the integral. We therefore assume that $U(y - \frac{Y}{k}) - U(y)$ vanishes only at $Y = 0$. In fact, a more general calculation could show that the result is also valid if $U(y - \frac{Y}{k}) - U(y)$ has more than one zero, but not on the critical point y_c . With this assumption we get

$$\begin{aligned} \mathcal{P} \left\{ \int dY e^{-|Y|} \frac{\cos(Y \tan \theta)}{U(y - \frac{Y}{k}) - U(y)} \right\} &= \lim_{\eta \rightarrow 0} \int_{-\eta}^{-\infty} dY e^{-|Y|} \frac{\cos(Y \tan \theta)}{U(y - \frac{Y}{k}) - U(y)} + \int_{\eta}^{+\infty} dY e^{-|Y|} \frac{\cos(Y \tan \theta)}{U(y - \frac{Y}{k}) - U(y)} \\ &= \int_0^{+\infty} dY e^{-|Y|} \cos(Y \tan \theta) \left\{ \frac{1}{U(y - \frac{Y}{k}) - U(y)} + \frac{1}{U(y + \frac{Y}{k}) - U(y)} \right\} \\ &= \int_0^{+\infty} dY e^{-|Y|} \cos(Y \tan \theta) \left\{ \frac{U(y - \frac{Y}{k}) + U(y + \frac{Y}{k}) - 2U(y)}{(U(y - \frac{Y}{k}) - U(y))(U(y + \frac{Y}{k}) - U(y))} \right\} \\ &\xrightarrow{K \rightarrow \infty} \frac{U''}{U'^2} \int_0^{+\infty} dY e^{-|Y|} \cos(Y \tan \theta) = \frac{U''}{U'^2} \frac{1}{1 + \tan^2 \theta}. \end{aligned}$$

We have used the relations $U(y - \frac{Y}{k}) + U(y + \frac{Y}{k}) - 2U(y) \sim U''' \frac{Y^2}{k^2}$ and $(U(y - \frac{Y}{k}) - U(y))(U(y + \frac{Y}{k}) - U(y)) \sim U'^2 \frac{Y^2}{k^2}$.

We have thus

$$\mathcal{R}e \langle v_\theta^* \omega_\theta \rangle \underset{K \rightarrow \infty}{\sim} -\frac{\hat{C}_{k,l}}{2k^2} \frac{U''}{U'^2} \frac{1}{1 + \tan^2 \theta} = -\frac{\hat{C}_{k,l}}{2K^2} \frac{U''}{U'^2}.$$

Finally, with the relation $\frac{1}{2} \iint dk' dl' \frac{\hat{C}_{k',l'}}{K'^2} = 1$ when we integrate over the whole spectrum, we get the desired result.

Appendix D. Modified Rossby waves

In this appendix, we discuss the neutral modes of parabolic jets $U(y) = \gamma \frac{y^2}{2}$.

We first note that for any parabolic jet, $U'' - \beta$ does not change sign. Hence the Rayleigh-Kuo criteria is satisfied and the jet has no unstable modes.

For a mean velocity $U(y) = \gamma \frac{y^2}{2}$, we are looking for solutions of (2.17) of the form $\omega_k(y) e^{-ikct}$. The equation writes

$$-ikc\omega_k + ik\gamma \frac{y^2}{2} \omega_k + ik(\beta - \gamma) H_k * \omega_k = 0.$$

We do the Fourier transform $\hat{\omega}_k(l) := \int dy \omega_k(y) e^{-ily}$ to obtain

$$-\frac{1}{2} \frac{d^2}{dl^2} \hat{\omega}_k + \frac{\mu}{k^2 + l^2} \hat{\omega}_k = \frac{c}{\gamma} \hat{\omega}_k, \quad (\text{D } 1)$$

where $\mu := 1 - \frac{\beta}{\gamma}$. We recognize the eigenvalue problem for a Schrödinger operator with a potential $\frac{\mu}{k^2 + l^2}$, a result already obtained by Brunet (Brunet 1990). Using classical results for this type of 1D Schrödinger equation, we can immediately conclude that

- There exists a solution $\hat{\omega}_k$ in L_2 iff $\mu < 0$ (attractive potential). In that case, the corresponding eigenvalue is negative which implies that $\frac{c}{\gamma} < 0$. The condition $\mu < 0$ imposes already $\gamma > 0$, so the phase velocity of Rossby wave is $c < 0$ and the wave is outside of the continuous spectrum. We find for this particular configuration the classical result that Rossby waves propagate with $c < U_{min}$.

- The number of modes $n(|\mu|)$ increases with $|\mu|$, the depth of the potential well. Modes organize into continuous families $\{\Omega_i(|\mu|)\}_{1 \leq i \leq n(|\mu|)}$, with energies $E_i(|\mu|) = \frac{c}{\gamma}$, when $|\mu|$ is changed. $E_i(|\mu|)$ are decreasing functions of $|\mu|$. The families Ω_i are alternatively even and odd function with a number of nodes that increases with i . A new set of modes appears for critical values μ_i . For $\mu = \mu_i$, the mode of the new family has a zero energy $E_i(|\mu_i|) = 0$.

To compute the eigenfunction of (D 1), for a given μ we use a bisection algorithm. We divide the interval $[\mu, 0]$ in sufficiently small intervals $[\tau_i, \tau_{i+1}]$ and compute the solution of (D 1) with $\frac{c}{\gamma} = \tau_i$. The solution diverges like an exponential at infinity, and when this divergence changes sign between τ_i and τ_{i+1} , it means that we have an eigenfunction in the interval, and we iterate the algorithm until $\tau_{i+1} - \tau_i$ is small enough. This way, we obtain the Fourier transform of a mode, we just have to inverse the Fourier transform to get the mode in real space. Then we project e^{ily} on these modes with the standard scalar product on L_2 . figure (12) displays the 3 first eigenfunctions obtained with $\mu = -1$.

REFERENCES

- ANDREWS, DG & MCINTYRE, ME 1978 Generalized eliasen-palm and charney-drazin theorems for waves on axisymmetric mean flows in compressible atmospheres. *Journal of the Atmospheric Sciences* **35** (2), 175–185.
- BAKAS, NIKOLAOS & IOANNOU, PETROS 2013 A theory for the emergence of coherent structures in beta-plane turbulence. *preprint arXiv:1303.6435*.
- BOUCHET, F. & MORITA, H. 2010 Large time behavior and asymptotic stability of the 2D Euler and linearized Euler equations. *Physica D Nonlinear Phenomena* **239**, 948–966, arXiv: 0905.1551.
- BOUCHET, FREDDY, NARDINI, CESARE & TANGARIFE, TOMÁS 2013 Kinetic theory of jet dynamics in the stochastic barotropic and 2d navier-stokes equations. *Journal of Statistical Physics* **153** (4), 572–625.
- BOUCHET, F, NARDINI, C & TANGARIFE, T 2016 Kinetic theory and quasilinear theories of jet dynamics. *arXiv preprint arXiv:1602.02879*, to be published in the book *Zonal Flows*, edited by Boris Galperin, and to be published by Cambridge University Press.
- BOUCHET, F. & SIMONNET, E. 2009 Random Changes of Flow Topology in Two-Dimensional and Geophysical Turbulence. *Physical Review Letters* **102** (9), 094504.
- BOUCHET, F. & VENAILLE, A. 2012 Statistical mechanics of two-dimensional and geophysical flows. *Physics Reports* **515**, 227–295.
- BRUNET, GILBERT 1990 *Dynamique des ondes de Rossby dans un jet parabolique..* Universite McGill.
- CONSTANTINOU, NAVID C 2015 Formation of large-scale structures by turbulence in rotating planets. *arXiv preprint arXiv:1503.07644*.
- CONSTANTINOU, NAVID C, IOANNOU, PETROS J & FARRELL, BRIAN F 2012 Emergence and equilibration of jets in beta-plane turbulence. *arXiv preprint arXiv:1208.5665*.

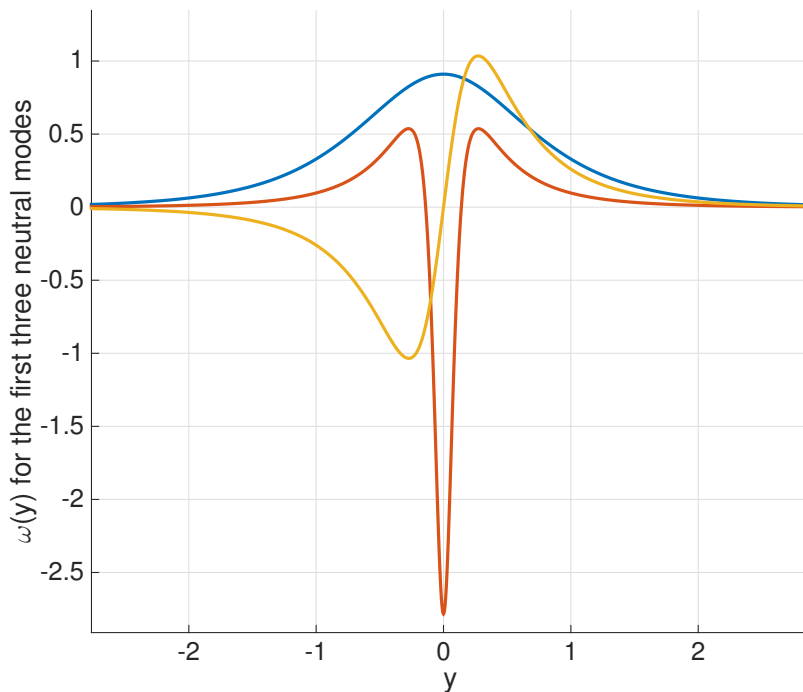


FIGURE 12. The first three neutral modes (modified Rossby waves) obtained for $\mu = -1$. Even modes and odd modes alternate. The first mode vanishes only at infinity, and each new mode has an additional zero.

- DRAZIN, PG, BEAUMONT, DN & COAKER, SA 1982 On rossby waves modified by basic shear, and barotropic instability. *Journal of Fluid Mechanics* **124**, 439–456.
- DRAZIN, PHILIP G & REID, WILLIAM HILL 2004 *Hydrodynamic stability*. Cambridge university press.
- DRITSCHER, D. G. & MCINTYRE, M. E. 2008 Multiple Jets as PV Staircases: The Phillips Effect and the Resilience of Eddy-Transport Barriers. *Journal of Atmospheric Sciences* **65**, 855.
- FALKOVICH, GREGORY 2016 Interaction between mean flow and turbulence in two dimensions. In *Proc. R. Soc. A*, , vol. 472, p. 20160287. The Royal Society.
- FARRELL, B. F. & IOANNOU, P. J. 1993 Stochastic Dynamics of Baroclinic Waves. *Journal of Atmospheric Sciences* **50**, 4044–4057.
- FARRELL, BRIAN F. & IOANNOU, PETROS J. 2003 Structural stability of turbulent jets. *Journal of Atmospheric Sciences* **60**, 2101–2118.
- FARRELL, B. F. & IOANNOU, P. J. 2007 Structure and Spacing of Jets in Barotropic Turbulence. *Journal of Atmospheric Sciences* **64**, 3652.
- FRISHMAN, ANNA, LAURIE, JASON & FALKOVICH, GREGORY 2017 Jets or vortices? what flows are generated by an inverse turbulent cascade? *Physical Review Fluids* **2** (3), 032602.
- GALPERIN, BORIS, SUKORIANSKY, SEMION & HUANG, HUEI-PING 2001 Universal n-5 spectrum of zonal flows on giant planets. *Physics of Fluids (1994-present)* **13** (6), 1545–1548.
- GALPERIN, BORIS, YOUNG, ROLAND MB, SUKORIANSKY, SEMION, DIKOVSKAYA, NADEJDA, READ, PETER L, LANCASTER, ANDREW J & ARMSTRONG, DAVID 2014 Cassini observations reveal a regime of zonostrophic macroturbulence on jupiter. *Icarus* **229**, 295–320.
- GARCÍ, E, SÁNCHEZ-LAVEGA, A & OTHERS 2001 A study of the stability of jovian zonal winds from hst images: 1995–2000. *Icarus* **152** (2), 316–330.

- GILL, ADRIAN E 1982 *Atmosphere-ocean dynamics*, , vol. 30. Academic press.
- INGERSOLL, ANDREW P 1990 Atmospheric dynamics of the outer planets. *Science* **248** (4953), 308–315.
- INGERSOLL, ANDREW P, BEEBE, RETA F, MITCHELL, JIM L, GARNEAU, GLENN W, YAGI, GARY M & MÜLLER, JAN-PETER 1981 Interaction of eddies and mean zonal flow on jupiter as inferred from voyager 1 and 2 images. *Journal of Geophysical Research A* **86** (A10), 8733–8743.
- KOLOKOLOV, IV & LEBEDEV, VV 2016a Structure of coherent vortices generated by the inverse cascade of two-dimensional turbulence in a finite box. *Physical Review E* **93** (3), 033104.
- KOLOKOLOV, IV & LEBEDEV, VV 2016b Velocity statistics inside coherent vortices generated by the inverse cascade of 2-d turbulence. *Journal of Fluid Mechanics* **809**.
- LAURIE, JASON, BOFFETTA, GUIDO, FALKOVICH, GREGORY, KOLOKOLOV, IGOR & LEBEDEV, VLADIMIR 2014 Universal profile of the vortex condensate in two-dimensional turbulence. *Physical review letters* **113** (25), 254503.
- LI, LIMING, INGERSOLL, ANDREW P & HUANG, XIANGLEI 2006 Interaction of moist convection with zonal jets on jupiter and saturn. *Icarus* **180** (1), 113–123.
- MARSTON, J. B., CONOVER, E. & SCHNEIDER, T. 2008 Statistics of an Unstable Barotropic Jet from a Cumulant Expansion. *Journal of Atmospheric Sciences* **65**, 1955, arXiv: 0705.0011.
- NARDINI, CESARE & TANGARIFE, TOMÁS 2016 Fluctuations of large-scale jets in the stochastic 2d euler equation. *arXiv preprint arXiv:1602.06720* .
- PEDLOSKY, JOSEPH 1964 The stability of currents in the atmosphere and the ocean: Part ii. *Journal of the Atmospheric Sciences* **21** (4), 342–353.
- PEDLOSKY, J. 1982 *Geophysical fluid dynamics*. New York and Berlin, Springer-Verlag, 1982. 636 p.
- PORCO, CAROLYN C, WEST, ROBERT A, McEWEN, ALFRED, DEL GENIO, ANTHONY D, INGERSOLL, ANDREW P, THOMAS, PETER, SQUYRES, STEVE, DONES, LUKE, MURRAY, CARL D, JOHNSON, TORRENCE V & OTHERS 2003 Cassini imaging of jupiter's atmosphere, satellites, and rings. *Science* **299** (5612), 1541–1547.
- READ, PL, YAMAZAKI, YH, LEWIS, SR, WILLIAMS, PAUL DAVID, MIKI-YAMAZAKI, K, SOMMERIA, JOËL, DIDELLE, HENRI & FINCHAM, A 2004 Jupiter's and saturn's convectively driven banded jets in the laboratory. *Geophysical research letters* **31** (22).
- REED, MICHAEL & SIMON, BARRY 1978 Modern methods of mathematical physics. *Analysis of Operators, Academic Press* .
- SALYK, COLETTE, INGERSOLL, ANDREW P, LORRE, JEAN, VASAVADA, ASHWIN & DEL GENIO, ANTHONY D 2006 Interaction between eddies and mean flow in jupiter's atmosphere: Analysis of cassini imaging data. *Icarus* **185** (2), 430–442.
- SÁNCHEZ-LAVEGA, A, ORTON, GS, HUESO, R, GARCÍA-MELENDO, E, PÉREZ-HOYOS, S, SIMON-MILLER, A, ROJAS, JF, GÓMEZ, JM, YANAMANDRA-FISHER, P, FLETCHER, L & OTHERS 2008 Depth of a strong jovian jet from a planetary-scale disturbance driven by storms. *Nature* **451** (7177), 437–440.
- SCHNEIDER, T. & LIU, J. 2009 Formation of Jets and Equatorial Superrotation on Jupiter. *Journal of Atmospheric Sciences* **66**, 579–, arXiv: 0809.4302.
- SOMMERIA, J. 1986 Experimental study of the two-dimensional inverse energy cascade in a square box. *Journal of Fluid Mechanics* **170**, 139–68.
- SRINIVASAN, KAUSHIK & YOUNG, WR 2014 Reynolds stress and eddy diffusivity of β -plane shear flows. *Journal of the Atmospheric Sciences* **71** (6), 2169–2185.
- SRINIVASAN, K. & YOUNG, W. R. 2011 Zonostrophic Instability. *Journal of the atmospheric sciences* **69** (5), 1633–1656.
- TANGARIFE, TOMÁS 2015 Kinetic theory and large deviations for the dynamics of geophysical flows. PhD thesis, Ecole normale supérieure de lyon-ENS LYON.
- VALLIS, GEOFFREY K & MALTRUD, MATTHEW E 1993 Generation of mean flows and jets on a beta plane and over topography. *Journal of physical oceanography* **23** (7), 1346–1362.
- VASAVADA, ASHWIN R & SHOWMAN, ADAM P 2005 Jovian atmospheric dynamics: An update after galileo and cassini. *Reports on Progress in Physics* **68** (8), 1935.
- WILLIAMS, GARETH P 1978 Planetary circulations: 1. barotropic representation of jovian and terrestrial turbulence. *Journal of the Atmospheric Sciences* **35** (8), 1399–1426.

WOILLET, E & BOUCHET, F 2017 Theoretical prediction of reynolds stresses and velocity profiles for barotropic turbulent jets. *EPL (Europhysics Letters)* **118** (5), 54002.